

Journal Pre-proof

A new hybrid model for wind speed forecasting combining long short-term memory neural network, decomposition methods and grey wolf optimizer

Aytaç Altan, Seçkin Karasu, Enrico Zio



PII: S1568-4946(20)30935-2
DOI: <https://doi.org/10.1016/j.asoc.2020.106996>
Reference: ASOC 106996

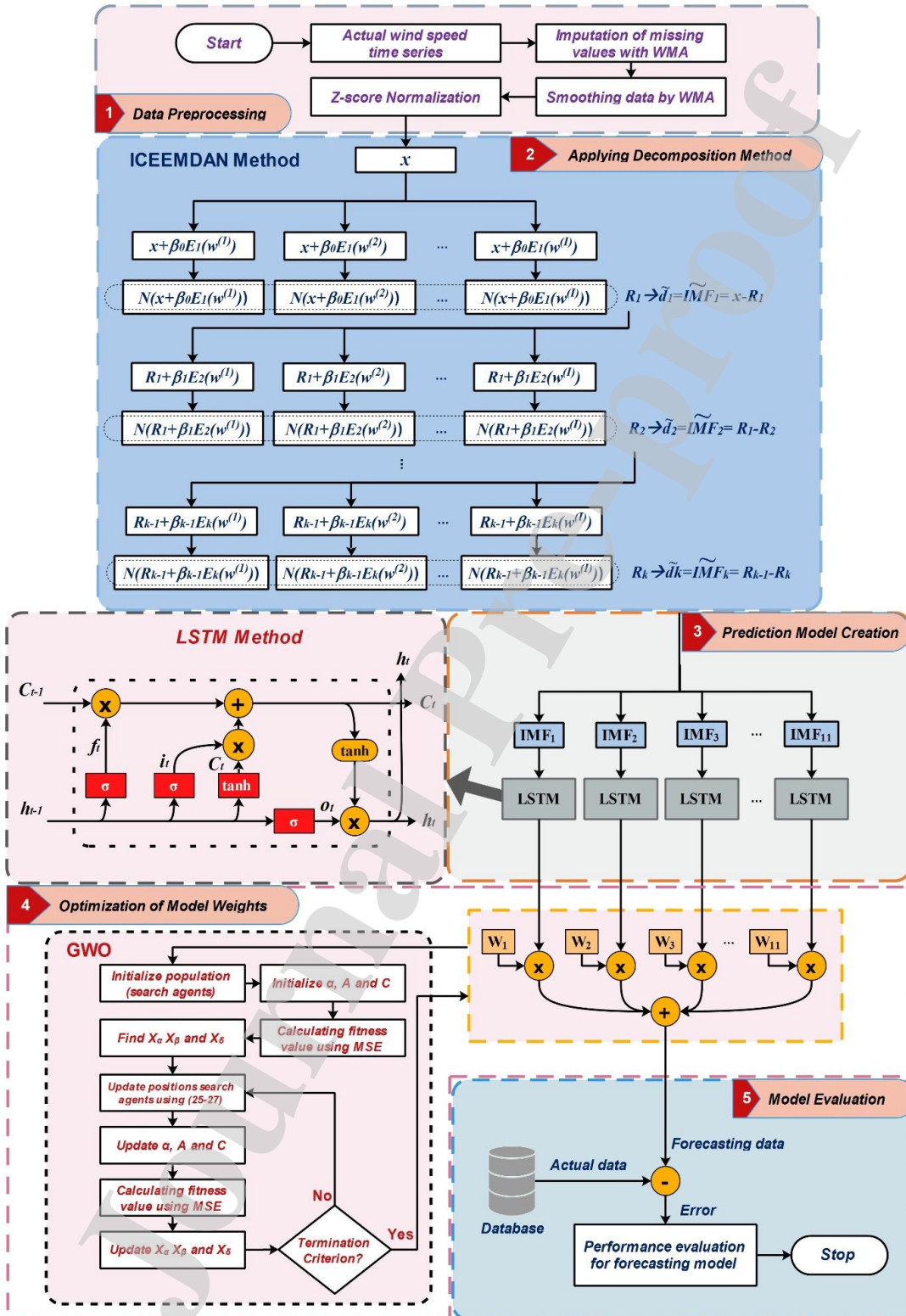
To appear in: *Applied Soft Computing Journal*

Received date : 9 December 2019
Revised date : 24 July 2020
Accepted date : 8 December 2020

Please cite this article as: A. Altan, S. Karasu and E. Zio, A new hybrid model for wind speed forecasting combining long short-term memory neural network, decomposition methods and grey wolf optimizer, *Applied Soft Computing Journal* (2020), doi: <https://doi.org/10.1016/j.asoc.2020.106996>.

This is a PDF file of an article that has undergone enhancements after acceptance, such as the addition of a cover page and metadata, and formatting for readability, but it is not yet the definitive version of record. This version will undergo additional copyediting, typesetting and review before it is published in its final form, but we are providing this version to give early visibility of the article. Please note that, during the production process, errors may be discovered which could affect the content, and all legal disclaimers that apply to the journal pertain.

© 2020 Elsevier B.V. All rights reserved.



1 **A new hybrid model for wind speed forecasting combining long short-term**
2 **memory neural network, decomposition methods and grey wolf optimizer**

3
4 Aytaç Altan^{a,*}, Seçkin Karasu^a, Enrico Zio^{b,c,d}

5
6 ^aDepartment of Electrical Electronics Engineering, Zonguldak Bülent Ecevit University,
7 67100 Zonguldak, Turkey

8 ^bMINES ParisTech, PSL Research University, CRC, Sophia Antipolis, France

9 ^cEnergy Department, Politecnico di Milano, Milan, Italy

10 ^dEminent Scholar, Department of Nuclear Engineering, College of Engineering, Kyung Hee
11 University, Republic of Korea

12 *Corresponding author e-mail: aytacaltan@beun.edu.tr

13
14 **Abstract**

15 Reliable and accurate wind speed forecasting (WSF) is fundamental for efficient exploitation
16 of wind power. In particular, high accuracy short-term WSF (ST-WSF) has a significant
17 impact on the efficiency of wind power generation systems. Due to the non-stationarity and
18 stochasticity of the wind speed (WS), a single model is often not sufficient in practice for the
19 accurate estimation of the WS. Hybrid models are being proposed to overcome the limitations
20 of single models and increase the WS forecasting performance. In this paper, a new hybrid
21 WSF model is developed based on long short-term memory (LSTM) network and
22 decomposition methods with grey wolf optimizer (GWO). In the pre-processing stage, the
23 missing data is filled by the weighted moving average (WMA) method, the WS time series
24 (WSTS) data are smoothed by WMA filtering and the smoothed data are used as model input
25 after Z-score normalization. The forecasting model is formed by the combination of a single
26 model, a decomposition method and an advanced optimization algorithm. Successively, the
27 hybrid WSF model is developed by combining the LSTM and decomposition methods, and

28 optimizing the intrinsic mode function (IMF) estimated outputs with a grey wolf optimizer
29 (GWO). The developed non-linear hybrid model is utilized on the data collected from five
30 wind farms in the Marmara region, Turkey. The obtained experimental results indicate that
31 the proposed combined model can capture non-linear characteristics of WSTS, achieving
32 better forecasting performance than single forecasting models, in terms of accuracy.

33 **Keywords:** wind speed, hybrid model, long short-term memory (LSTM), decomposition, grey
34 wolf optimizer (GWO).

35

36 1. Introduction

37 Renewable energy is experiencing great developments at the global level with the highest
38 growth of wind and solar photovoltaic, specifically 27% annual growth and 42% annual
39 growth over the last decade, respectively [1]. The installed power of renewable energy has
40 reached 2351 Gigawatts (GW) worldwide in 2018. In the European Union (EU), the installed
41 capacity has reached 536 GW in 2018 [2]. It is expected that the contribution of renewable
42 energy to electricity generation in the EU will continue to increase and reach 1210 Terawatts
43 (TW) hours in 2020. This amounts to approximately 34% of gross final electricity
44 consumption by 2020 [3]. In particular, wind energy, one of the renewable energy sources, is
45 growing rapidly in recent years. By the end of 2018, the total power capacity of all the wind
46 turbines installed in the world reached 597 GW, according to the World Wind Energy
47 Association [4]. It is foreseen that wind energy will be the most important renewable energy
48 source and provide approximately 40% of all renewable electricity by 2020 [3]. Developing
49 wind energy technology is, thus, expected to provide substantial support to traditional energy
50 sources in the future. In order to be able to benefit from wind energy technology, it is very
51 important to know the possibilities of its utilization, i.e., to determine regions with high
52 potential of wind energy, and to predict the wind characteristics and speeds. For Turkey, in
53 particular, it is estimated that the wind energy potential amounts to about 50,000 MW

54 whereas the installed capacity is only around 10% of this value [5]. The accurate modeling of
55 the wind regime based on its statistical properties like humidity, temperature, solar radiation,
56 pressure and WS is very important in order to use the existing potential in the region.

57

58 Accurate WSF, in particular, is critical to wind farm design and operation [6]. Existing
59 methods can be roughly divided into two kinds, as forecasting and optimization methods are
60 used to develop the WSF models. The forecasting methods are used as the predictors to
61 perform WSF, and they include physical, statistical, artificial intelligence (AI), and hybrid
62 models. Optimization methods, including signal processing with optimization of the
63 parameters, are used to improve the forecasting [7, 8].

64

65 Physical models are used to estimate long-term WS using physical data such as terrain,
66 obstacle, roughness, atmospheric pressure and ambient temperature [9, 10]. These models are
67 occasionally used as the first step to predicting the wind ancillary input of other statistical
68 models [9]. Models like numerical weather forecast (NWF) [11], mesoscale model 5 (MM 5)
69 [12], weather research and forecast (WRF) [13], model output statistics (MOS) and Eta model
70 [14], high resolution model (HRM) [15], often combine multiple physical considerations to
71 provide satisfactory prediction accuracy. However, these models are not convenient for ST-
72 WSF, because of the high costs and complexity of the calculation [16].

73

74 Statistical methods, are usually preferred for ST-WSF, and employ historical data to estimate
75 WS. The model parameters are adjusted to minimize the error between the actual and the
76 estimated WS data [16, 17]. Among the statistical methods, used for WSF there are both
77 linear and nonlinear models. Common linear statistical models for WSF include the auto-
78 regressive (AR) [18], linear regression [19], moving average (MA) [20], Kalman filtering [23,
79 24], ARMA [21], Markov chain [25] and AR integrated MA (ARIMA) [22] models. If the

80 nonlinear characteristics are prominent, however, the forecasting results by these models may
81 not be satisfactory for the intended application [26]. This is often the case in practice for wind
82 speed time series (WSTS) [27]. In this case, non-linear statistical models for WSF perform
83 better, which include nonlinear auto regressive (NAR) and nonlinear auto regressive
84 exogenous (NARX) models [28-30]. In [19], an AR model that is sufficiently flexible for
85 modeling the main features of WS and sufficiently sensitive for wind turbines has been used.
86 Riahy and Abedi [20] proposed a linear MA prediction model for ST-WSF. A window is
87 utilized to estimate the future samples of WS. Erdem and Shi [21] applied four different
88 ARMA models for the estimation of WS and direction. In [22], the fractional ARIMA has
89 been employed for the prediction of WS on one day and two day-ahead horizons. Cadenas et
90 al. [29] performed one-step ahead forecasting of the next WS with ARIMA and NARX
91 models for two different regions. In addition to WS from meteorological data, average values
92 of temperature, pressure, solar radiation and humidity data were used for both regions. The
93 NARX model performed better than the ARIMA model for both regions. In [31], a new WSF
94 model was developed by using AR with Hammerstein models. Akçay and Filik [32] built a
95 Kalman filter for one-and multi-step ahead WSF.

96
97 AI methods are also effectively used to estimate WS. These methods include various types of
98 artificial neural networks (ANNs), like [33], multi-layer perceptron (MLP) [34], back
99 propagation neural network (BPNN) [35], long short term memory (LSTM) [36], radial basis
100 function (RBF) [37], recurrent neural network (RNN) [38], Elman neural network (ENN)
101 [39], **convolutional neural network (CNN)** [40] and wavelet neural network (WNN) [41], and
102 also fuzzy logic (FL) methods [42]. There exist various implementations of AI methods for
103 WSF in the literature. Modandes et al. [43] proposed the use of a support vector machine
104 (SVM) to predict short term WS (ST-WS) by using daily average data of WS. Guo et al. [44]
105 have focused on a new combined approach based on seasonal exponential adjustment and

106 BPNN, which effectively improves the WS forecasting accuracy. In [45], a hybrid wavelet
107 neural network (WNN) has been developed, based on the multi-objective sine cosine
108 algorithm (MOSCA) for achieving strong stability and high accuracy simultaneously. In [41,
109 46], two types of deep learning model based on the LSTM network for one and multi-step
110 WSF have been developed.

111

112 More in general, machine learning algorithms are often used for WSF, including SVM, K-
113 nearest neighbor (KNN), adaptive boosting (Adaboost) and evolutionary algorithms for
114 parameter optimization [47]. Kiplangat et al. [48] have developed a data-driven multi-model
115 WSF technique by using a two-layer ensemble machine learning method. For the purpose of
116 establishing a more generalized estimation model, the deep feature selection approach is used
117 for meteorological data (temperature, pressure, humidity, etc.). The proposed multi-model
118 WSF technique is compared with single models and it is observed that the ST-WSF
119 performance is enhanced. In [49], SVM models for short-term accurate prediction of WS have
120 been proposed.

121

122 In WSF, the models that use a combination of forecasting and optimization techniques are
123 called hybrid or combined models. Recently, hybrid (combined) models have been used
124 frequently for WSF. In [50], a hybrid model based on Adaboost-extreme learning machine
125 (AELM) with two-stage decomposition is proposed and applied to four WS data sets for one-
126 two-and three-step ahead prediction. In [51], a hybrid model based on environmental factors
127 for ST-WSF is developed using SVM and wavelet transform (WT), which is optimized by
128 genetic algorithm (GA). In [52], a hybrid model has been proposed, combining regularized
129 ELM (RELM) network, empirical wavelet transform (EWT) decomposition, inverse empirical
130 wavelet transform (IEWT) reconstruction and grey wolf optimizer (GWO) algorithm. The WS
131 data is divided into time series components by the EWT decomposition. The parameters of the

132 RELM network are optimized by GWO. The RELM network optimized by GWO is used to
133 estimate each sub-time series. The IEWT is used as a filter bank to avoid unsuspected
134 prediction values and reconstruct the predicted results. In [53], a hybrid model called
135 EnsemLSTM has been proposed, which has deep learning time series estimation based on
136 LSTMs, extremal optimization (EO) algorithm and support vector regression machine
137 (SVRM). The estimation values of LSTMs are collected into the top layer of a non-linear
138 learning regression composed of SVRM, and the ST-WS is forecasted by SVRM with model
139 parameters that are optimized by EO. Hu et al. [54] have developed a non-linear hybrid model
140 that aims to improve WSF accuracy by combining LSTM, differential evolution (DE), non-
141 linear hybrid mechanism and hysteretic ELM (HELM). The DE algorithm is used to optimize
142 the LSTM model successfully, while balancing its complexity. Wang et al. [55] have
143 developed a hybrid model for ST-WSF, which combines an improved complementary
144 ensemble empirical mode decomposition with adaptive noise (ICEEMDAN), ARIMA and
145 ELM. The ELM model is utilized for ST-WSF, whilst the ARIMA model is employed to
146 specify the best input variables. The robustness of the ELM is increased using the ensemble
147 method. It is pointed out that the proposed model is more robust than other versions of
148 empirical mode decomposition (EMD) in achieving nonstationary decomposition, and
149 provides satisfactory performance for both pre-processing and post-processing. Jiang and
150 Huang [56] proposed a hybrid model that includes attribute selection and error correction
151 steps to enhance the achievement of decomposition-based estimation models used in real-time
152 WSF. The WSTS is separated into a number of different sub-series by ensemble EMD
153 (EEMD) method. Kullback-Leibler divergence based on kernel density prediction and feature
154 selection method based on energy measurement are applied. The error components are
155 corrected by combination of the generalized AR conditionally heteroscedastic and least
156 squares SVM.

157

158 In this study, we propose a new modeling framework for WSF. The elements of the proposed
159 hybrid WSF modeling framework include filling the missing data, normalization by Z-score,
160 creating a forecasting model by combining the LSTM and decomposition method, and
161 optimizing the intrinsic mode function (IMF) predicted outputs with GWO. The proposed
162 hybrid model is called ICEEMDAN-LSTM-GWO. The remainder of this paper is organized
163 as follows. In Section 2, the specific methodology is introduced, including the data pre-
164 processing method, optimization method, and proposed hybrid model. The experimental
165 procedure and analysis are presented in Section 3. In Section 4, some tangible discussions are
166 presented to prove the performance of the new hybrid model. Finally, conclusions are
167 highlighted in Section 5.

168 **2. ICEEMDAN-LSTM-GWO hybrid WSF modeling framework**

169 In this section, the specific methods composing the developed ICEEMDAN-LSTM-GWO
170 hybrid model for WSF, namely data preprocessing, LSTM neural network, ICEEMDAN
171 technique and GWO algorithm, are presented. In extreme synthesis, a forecasting model is
172 created with LSTM neural network for each of the IMF obtained by ICEEMDAN technique,
173 and the weight coefficients of each output are optimized with GWO.

174 *2.1 Data pre-processing*

175 The WSTS data are pre-processed before being fed to the proposed hybrid model. In the pre-
176 processing step, the missing data are filled by means of a weighted moving average (WMA)
177 method. The WSTS data are smoothed by WMA filtering and the normalization of the
178 smoothed data is done by *Z-score* normalization. The methods used in the data pre-processing
179 phase are described in the following sections.

180 *2.1.1 Imputation of missing data*

181 The missing data of some measurements due to sensor malfunctions or to the nature of the
182 wind can cause significant deterioration of the wind power system's model performance.

183 When some measurements are missing, the forecasting accuracy is generally offset by
 184 gathering data over long horizons. In literature, interpolation, Kalman filters, persistence,
 185 WMA, random sample approaches are frequently used in the imputation process [57]. In this
 186 study, the missing data are filled with a simple WMA approach for imputation.

187 2.1.2 *Weighted moving average*

188 In the WMA method, each of the missing values is filled with the mean of the k -observation,
 189 which is a window of k data samples on both sides of the missing value [57].

190 For example, the one-step ahead WMA forecast is

$$\hat{Y}_{t+1} = \sum_{-k}^k \omega_i Y_{t+1+i} \quad (1)$$

191 where Y_t is the time series of interest for $t = 1, \dots, T$ and $\omega_{-k}, \omega_{-k+1}, \dots, \omega_k$ are the weights.

192 The window size k is increased incrementally when the complete window is void because of
 193 missing values. The weights are linearly decreasing in time as $1/2, 1/3, 1/4, \dots$ till the end of
 194 the window.

195 2.1.3 *Z-score normalization*

196 The Z -score, which is calculated using the standard deviation and arithmetic mean of the
 197 given WS data, is frequently used as score normalization technique. It is expected that this
 198 normalization technique will perform well in case of prior knowledge about the average score
 199 and the score variations of the matcher [58]. The normalized scores are given by

$$s'_k = \frac{s_k - \mu}{\sigma} \quad (2)$$

200 where σ is the standard deviation and μ is the arithmetic mean of the given data. In this study,
 201 the normalization of the smoothed data is done by Z -score normalization.

202 2.2 *Decomposition techniques*

203 The EMD technique is an adaptive method introduced to analyze non-linear and nonstationary
 204 signals [59]. The basis of the method is to empirically define internal oscillation modes with

205 characteristic time scales in the data and, then, to decompose the data accordingly. In fast and
 206 slow oscillations, it involves the decomposition of a signal locally and fully in a data-driven
 207 manner, through a sifting process. The ensemble EMD (EEMD) technique has been proposed
 208 to alleviate the problem of very similar oscillations in different modes, called "mode mixing",
 209 that are often a consequence of signal intermittency, in physical applications. The EEMD
 210 consists of a data decomposition ensemble that is appended to different realizations of the
 211 finite amplitude white noise and, then, takes the means of the corresponding IMFs from
 212 different decompositions as the final result [60, 61]. EEMD defines the "true" IMF
 213 components as the average of the corresponding IMFs obtained via EMD over an ensemble of
 214 trials, generated by adding different realizations of white noise of finite variance to the
 215 original signal $x[n]$. The EEMD algorithm can be defined as [62]:

- 216 (i) generate $x^{(i)} = x + \beta w^{(i)}$, where $w^{(i)}$ ($i = 1, \dots, I$) are different realizations of
 217 white Gaussian noise (WGN) and $\beta > 0$,
- 218 (ii) each $x^{(i)}$ ($i = 1, \dots, I$) is completely decomposed by EMD, obtaining the modes
 219 $d_k^{(i)}$, where $k = 1, \dots, K$ are the modes,
- 220 (iii) take \bar{d}_k as the k th mode of x , obtained as the mean of the corresponding modes

$$\bar{d}_k = \frac{1}{I} \sum_{i=1}^I d_k^{(i)} \quad (3)$$

221 In the EEMD, it can be recognized that every x^i is decomposed independently from the other
 222 realizations and for every one of them a residue $R_k^i = R_{k-1}^i - d_k^i$ is obtained at each stage,
 223 without any link between the different realizations. The reconstructed signal contains residual
 224 noise and different realizations of signal plus noise may produce a different numbers of
 225 modes. The complete EEMD with adaptive noise (CEEMDAN) technique is proposed to
 226 overcome these situations [62]. The full reconstruction of the original signal and an improved
 227 spectral separation of the modes with lower computational cost are achieved by the

228 CEEMDAN technique. In this method, a certain amount of noise is added at each phase of
 229 decomposition, and a unique residue is calculated to obtain each mode. The resulting
 230 dissociation is complemented by a numerically negligible error. However, there are still
 231 problems with some residual noise and “spurious” modes. The ICEEMDAN technique is
 232 developed to improve the problems with some residual noise and ”spurious“ modes by
 233 Colominas et al. [63]. This technique introduces operator $E_k(\cdot)$ and $N(\cdot)$. Let $E_k(\cdot)$ be the
 234 operator which produces the k th mode obtained by EMD, $N(\cdot)$ be the operator which
 235 produces the local average of the signal, and w^i a realization of WGN with zero mean and
 236 unit variance. The ICEEMDAN technique can be defined by the following steps:

237 (i) compute by EMD the local means of I realizations

$$x^{(i)} = x + \beta_0 E_1(w^{(i)}), \quad i = 1, \dots, I \quad (4)$$

238 where $\beta_0 = \varepsilon_0 \text{std}(x) / E_1(w^{(i)})$, and ε_0 is defined as reciprocal of the desired signal to noise
 239 ratio (SNR) between the first added noise and the analyzed signal,

240 (ii) compute the first residue R_1

$$R_1 = \langle N(x^{(i)}) \rangle \quad (5)$$

241 where $\langle \cdot \rangle$ is the action of averaging throughout the realizations,

242 (iii) calculate the first mode at the first stage ($k = 1$)

$$\tilde{d}_1 = x - R_1 \quad (6)$$

243 (iv) predict the second residue as the mean of the local means of the realizations

$$R_1 + \beta_1 E_2(w^{(i)}) \quad (7)$$

244 and describe the second mode as

$$\tilde{d}_2 = R_1 - R_2 = R_1 - \langle N(R_1 + \beta_1 E_2(w^{(i)})) \rangle \quad (8)$$

245 (v) for $k = 3, \dots, K$, compute the k th residue

$$R_k = \langle N(R_{k-1} + \beta_{k-1} E_k(w^{(i)})) \rangle \quad (9)$$

247 where β_k is chosen as $\beta_k = \varepsilon_0 \text{std}(R_k)$, $k \geq 1$ to obtain the desired SNR between the added
 248 noise and the residue,

249 (vi) compute the k th mode

$$\tilde{d}_k = R_{k-1} - R_k \quad (10)$$

250 (vii) go back to step (v) for next k .

251 2.3 Long short term memory network

252 LSTM network, a special type of RNNs, has a strong ability to solve long-term and short-term
 253 dependence problems with its success in the processing of non-linear sequential data. The
 254 core of the LSTM network is the memory cell that replaces the hidden layers of conventional
 255 neurons [64]. The LSTM network can add or remove information from the *input gate*, *output*
 256 *gate*, and *forget gate* to the memory cell state. This structure provides the LSTM with the
 257 ability to determine which cells are suppressed and stimulated based on the previous state,
 258 current memory and current input. The vanishing gradient problem is effectively overcome
 259 by this structure, shown in Fig. 2, such that the neural networks can recall information from a
 260 long range. In order to identify new information that can be collected in the cell, the input data
 261 is multiplied by the output of the input gate. To calculate the information that can be spread to
 262 the network, the output data for the network is multiplied by the activation of the output gate.
 263 To determine whether the last state of the cell should be forgotten, the cell states of the
 264 previous time are multiplied by the activation of the forget gate [65]. The procedure of the
 265 LSTM [66] is as follows:

266 • the stage of deciding what information to be discarded from the cell state: the value of
 267 x_t and h_{t-1} is obtained, and determines whether to discard through a sigmoid function:

$$f_t = \sigma(W_f \cdot [h_{t-1}, x_t] + b_f) \quad (11)$$

268 • the stage of determining which new information is stored in the cell state: it is decided
 269 by a sigmoid layer which information will be stored in the cell state; then, the values obtained
 270 from the $\tanh(\cdot)$ layer by x_t and h_{t-1} are taken as a new candidate value \tilde{C}_t :

$$i_t = \sigma(W_i \cdot [h_{t-1}, x_t] + b_i) \quad (12)$$

$$\tilde{C}_t = \tanh(W_C \cdot [h_{t-1}, x_t] + b_C) \quad (13)$$

271 • the step of updating the previous cell state C_{t-1} to the new cell state C_t : the cell state
 272 C_{t-1} is multiplied by f_t to forget what information we decide to forget. Then, to obtain a new
 273 cell state C_t , i_t is multiplied by \tilde{C}_t and new cell state C_t is determined by adding the term
 274 obtained to the previous term.

$$C_t = f_t * C_{t-1} + i_t * \tilde{C}_t \quad (14)$$

275 • the stage of deciding what information will be output: it is decided by a sigmoid layer
 276 which information will be output in the cell state.

$$o_t = \sigma(W_o \cdot [h_{t-1}, x_t] + b_o) \quad (15)$$

$$h_t = o_t * \tanh(C_t) \quad (16)$$

277 where W_f, W_i, W_C, W_o denote the weight matrices, b_f, b_i, b_C, b_o represent the bias vectors,
 278 respectively; $\sigma(\cdot)$ is the logistic sigmoid function which is utilized as the gate activation
 279 function:

$$\sigma(x) = \frac{1}{1 + e^{-x}} \quad (17)$$

280 and $\tanh(\cdot)$ is a hyperbolic tangent function used as activation function of the input and
 281 output blocks:

$$\tanh(x) = \frac{e^x - e^{-x}}{e^x + e^{-x}} \quad (18)$$

282
 283 2.4 *Grey wolf optimizer algorithm*

284 The GWO is a new and effective meta-heuristic optimization algorithm, which is a swarm
 285 intelligence-based evolutionary computation method based on the simulation of the hunting

286 behavior and social leadership of grey wolves in nature [67]. In this algorithm, inspired by
 287 grey wolves, the grey wolf's leadership and hunting mechanisms are imitated. Four types of
 288 grey wolves, alpha (α), beta (β), delta (δ) and omega (ω), are applied to imitate the
 289 leadership hierarchy. The nature of the GWO algorithm is that α , β , and δ wolves guide the
 290 optimization process, while being followed by ω wolves. The main stages of the grey wolf
 291 hunting are [68]:

- 292 • chasing, approaching, and tracking prey
- 293 • pursuing, harassing, and encircling the prey
- 294 • stationary wait and attack towards the prey.

295 The hunting behavior of grey wolves is shown in Fig. 1. The stage of the chasing,
 296 approaching, and tracking of the prey is shown in Fig. 1(A); the stages of the pursuing,
 297 harassing, and encircling of the prey are shown in Fig. 1(B-D); the stages of the stationary
 298 wait and attack towards the prey are shown in Fig. 1(E). The encircling behavior of a grey
 299 wolf throughout hunting is modeled as [69, 70]

$$\vec{D} = |\vec{C} \cdot \vec{X}_p(t) - \vec{X}(t)| \quad (19)$$

$$\vec{X}(t+1) = \vec{X}_p(t) - \vec{A} \cdot \vec{D} \quad (20)$$

300 where t shows the current iteration, \vec{A} and \vec{C} are coefficient vectors, $\vec{X}(t)$ and $\vec{X}_p(t)$ are
 301 position vectors of grey wolf and prey, respectively. The vector \vec{A} and \vec{C} are calculated as

$$\vec{A} = 2\vec{a} \cdot \vec{r}_1 - \vec{a} \quad (21)$$

$$\vec{C} = 2 \cdot \vec{r}_2 \quad (22)$$

303 where \vec{r}_1 and \vec{r}_2 are random vectors in $[0, 1]$ and the \vec{a} components are linearly decreased
 304 from 2 to 0 over the course of iterations.

305

306 Grey wolves have the capability to recognize the position of the prey and encircle it. To
 307 mathematically simulate the hunting behavior of grey wolves, α , which is the best candidate

308 solution, β , and δ are presumed to have a better knowledge of the potential position of the
 309 prey. This process is defined with the help of the following mathematical formulas as

$$\vec{D}_\alpha = |\vec{C}_1 \cdot \vec{X}_\alpha - \vec{X}|, \vec{D}_\beta = |\vec{C}_2 \cdot \vec{X}_\beta - \vec{X}|, \vec{D}_\delta = |\vec{C}_3 \cdot \vec{X}_\delta - \vec{X}| \quad (23)$$

$$\vec{X}_1 = \vec{X}_\alpha - \vec{A}_1 \cdot (\vec{D}_\alpha), \vec{X}_2 = \vec{X}_\beta - \vec{A}_2 \cdot (\vec{D}_\beta), \vec{X}_3 = \vec{X}_\delta - \vec{A}_3 \cdot (\vec{D}_\delta) \quad (24)$$

$$\vec{X}(t+1) = \frac{\vec{X}_1 + \vec{X}_2 + \vec{X}_3}{3} \quad (25)$$

310 where t indicates the current iteration, $\vec{A}_1, \vec{A}_2, \vec{A}_3$ are random vectors, and $\vec{X}_\alpha, \vec{X}_\beta$ and \vec{X}_δ
 311 indicate the position of α, β and δ wolves, respectively.



312

313

Fig. 1. Hunting behavior of grey wolves [68].

314 When the movement of the prey stops, the grey wolves finish the hunt with an attack. The
 315 value of \vec{a} is decreased for the mathematical model approaching its prey. At that time, the
 316 fluctuation range of \vec{A} is also decreased by \vec{a} . The next position of a search agent could be any
 317 position between its current position and the position of the prey. The grey wolves that have
 318 diverged from each other to search for their prey and converge to attack the prey, mostly
 319 search according to the position of α, β and δ . For mathematical model divergence, the search
 320 agent must be diverged from the prey with random values greater than 1 or less than -1. The
 321 GWO algorithm is shown in Fig. 2.

322 *2.5 Framework of the developed ICEEMDAN-LSTM-GWO hybrid model for WSF*

323 In this study, the ingredients of the novel combined modelling framework for WSF consist of
324 data preprocessing phase, a novel forecasting model creation phase by combining the LSTM
325 and ICEEMDAN decomposition method, the phase of optimizing IMF predicted outputs with
326 GWO and the phase of model evaluation.

327 *2.5.1 Data preprocessing phase*

328 In the data preprocessing phase, the missing data are filled with the WMA method and the
329 WSTS data are smoothed by WMA filter. Also in this phase, the normalization of the
330 smoothed data is done by Z-score normalization before the training and testing phases of the
331 proposed hybrid model.

332 *2.5.2 ICEEMDAN-LSTM combined forecasting model creation phase*

333 In this phase of the study, IMFs are obtained by the ICEEMDAN decomposition method. In
334 order to eliminate noise signals and stochastic volatility, the ICEEMDAN method
335 decomposes the original series and reconstructs the filtered time series. For each output of the
336 IMFs, a combined forecasting model is established with LSTM network and ICEEMDAN.
337 The processed WS data obtained at the end of this phase will be used for the next phase of
338 optimization. In LSTM model, the number of hidden unit is set to 500 and the maximum
339 epoch is set to 300.

340 *2.5.3 Optimization phase*

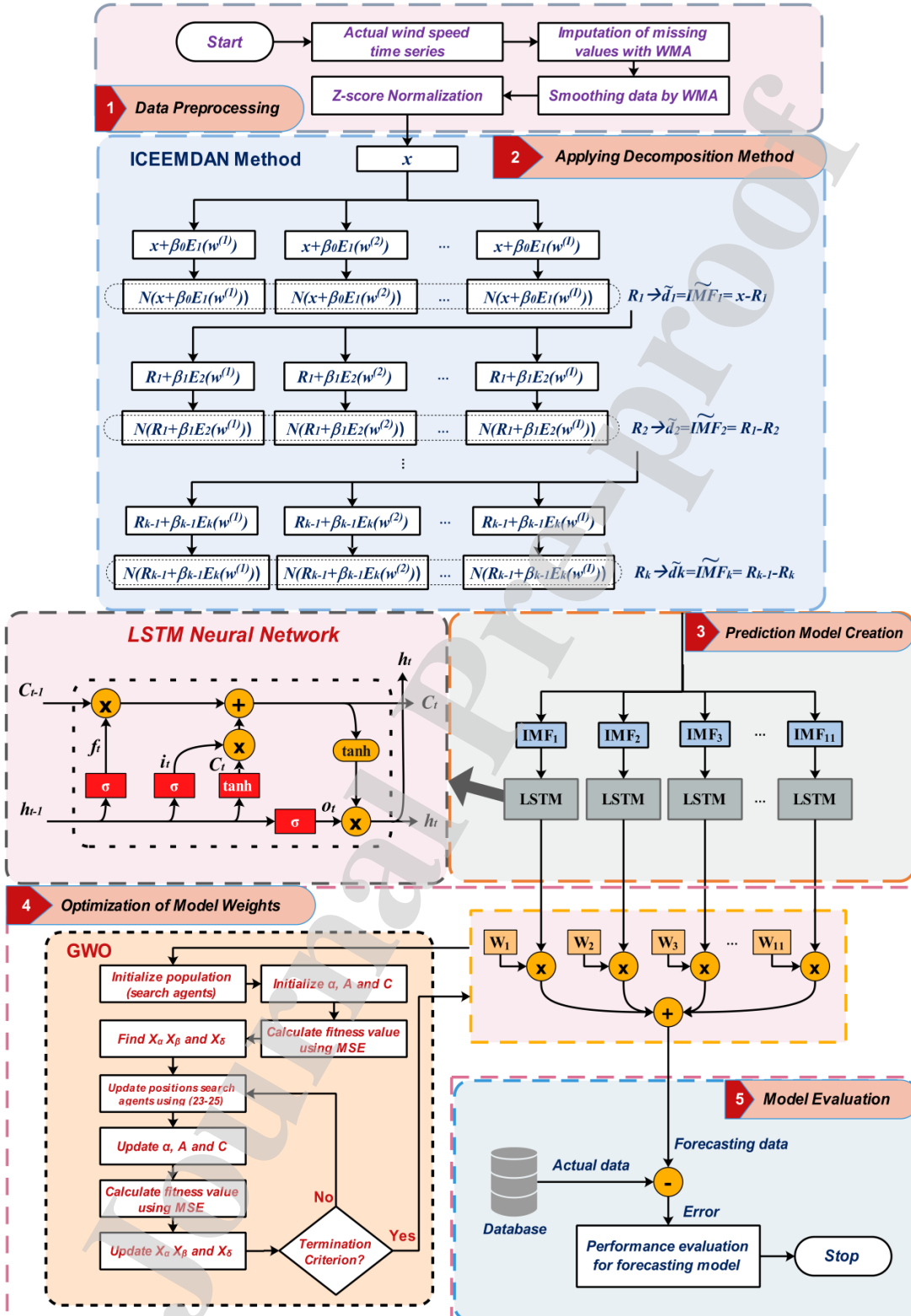
341 The weighted coefficients of each IMF output are optimized to create the best forecasting
342 model with the GWO algorithm. The objective function is the mean square error (MSE).

343 *2.5.4 Model evaluation phase*

344 The performance of the new hybrid model is measured by considering the mean absolute error
345 (MAE), root mean square error (RMSE) and mean absolute percentage error (MAPE) values.

346

347



348

349

Fig. 2. Process for the development of the ICEEMDAN-LSTM-GWO hybrid WSF model.

350 The formulas of the three error metrics are presented in Table 1. The MAE and RMSE are
 351 used to assess the average difference between the actual and the forecasted values. MAPE is
 352 defined as the mean of the absolute error.

353 **Table 1**

354 Error metrics for WSF model evaluation.

Metric	Description	Formula
MAE	Mean absolute error	$MAE = \frac{1}{N} \sum_{i=1}^N p_{predicted}^i - p_{actual}^i $
MAPE	Mean absolute percentage error	$MAPE = \frac{1}{N} \sum_{i=1}^N \left \frac{p_{actual}^i - p_{predicted}^i}{p_{actual}^i} \right \times 100\%$
RMSE	Root mean square error	$RMSE = \sqrt{\frac{1}{N} \sum_{i=1}^N (p_{predicted}^i - p_{actual}^i)^2}$

355

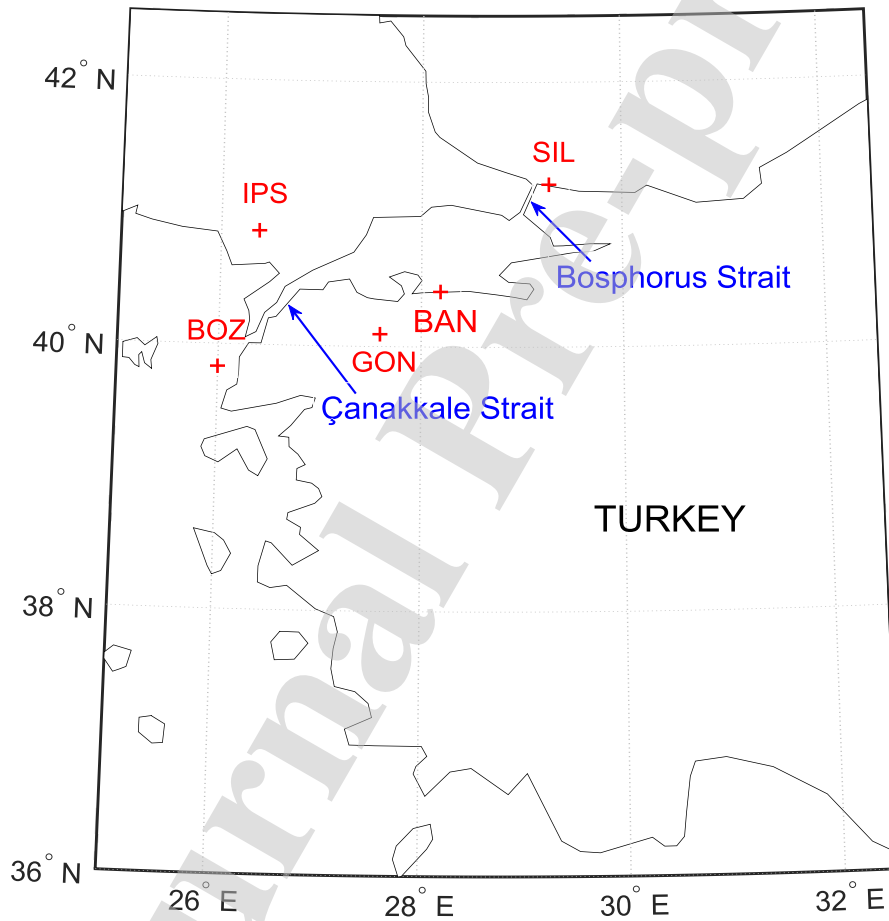
356 3. Experimental procedure and analysis

357 In this section, the studies performed with data collected from five wind farms in the Marmara
 358 region and the developed ICEEMDAN-LSTM-GWO hybrid WSF model are presented. The
 359 developed ICEEMDAN-LSTM-GWO hybrid WSF model is compared with other models
 360 obtained by combining with different decomposition methods. Moreover, the effect of GWO
 361 on the combined models is investigated.

362 3.1 Wind speed datasets

363 The WS data used in this study are collected from five different meteorological stations
 364 around the Marmara region in Turkey. The region where the data is collected is one of the
 365 highest potential wind energy locations of Turkey. The stations of Bandırma (BAN),
 366 Bozcaada (BOZ), Gönen (GON), İpsala (IPS) and Şile (SIL) are chosen arbitrarily among the
 367 available measurement locations in the region (Fig. 3). Each measurement location is isolated
 368 from the others and is not near the Çanakkale and Bosphorus Straits. The WS and direction
 369 measurements are collected between 2008 and 2014, for a period of 6 and 2/3 years.

370 Approximately 52,000 hours of WS measurement data are collected from each station. The
371 10-hour average of the collected data is taken and 15% of the data set is allocated as test data.
372 Some statistical values of the five WS datasets are given in Table 2, including standard
373 deviation, minimum, mean and maximum. The validity of the experimental data obtained
374 from five wind stations is evaluated by uncertainty analysis [71]. The upper and lower
375 confidence levels for the forecasting values are determined by uncertainty analysis.



376
377 **Fig. 3.** Five meteorological stations in Marmara region of Turkey.
378
379
380
381
382
383

384 **Table 2**

385 Statistical values of the five WS datasets.

Dataset	Samples	Numbers	Statistical values (m/s)			
			Min	Max	Mean	Std.
BOZ	All samples	5173	0.5	30.5	5.8528	3.1660
	Training	4397	0.7	30.5	5.9617	3.2106
	Testing	775	0.5	17.5	5.2316	2.8233
IPS	All samples	5173	0.3	14.9	2.8671	1.5143
	Training	4397	0.3	14.9	2.9177	1.5406
	Testing	775	0.4	10.9	2.5785	1.3203
GON	All samples	5173	0.4	13.4	2.0611	1.2411
	Training	4397	0.4	13.4	2.0759	1.2540
	Testing	775	0.4	6.8	1.9760	1.1627
BAN	All samples	5173	0.6	25.7	3.9893	2.5093
	Training	4397	0.7	25.7	4.0370	2.5426
	Testing	775	0.6	11.6	3.7145	2.2926
SIL	All samples	5173	0.1	12.9	2.2089	1.0840
	Training	4397	0.1	12.9	2.2517	1.1197
	Testing	775	0.6	5.7	1.9655	0.8132

386

387 *3.2 Experimental results and analysis*

388 The developed hybrid model combines the ICEEMDAN, LSTM and GWO and is applied to
389 the five WSTS, together with seventeen other WSF models. These are single NAR model
390 (Appendix A), single LSTM model, EMD-NAR combined model, EEMD-NAR combined
391 model, CEEMDAN-NAR combined model, ICEEMDAN-NAR combined model, EMD-
392 NAR-GWO combined model, EEMD-NAR-GWO combined model, CEEMDAN-NAR-
393 GWO combined model, ICEEMDAN-NAR-GWO combined model, EMD-LSTM combined
394 model, EEMD-LSTM combined model, CEEMDAN-LSTM combined model, ICEEMDAN-
395 LSTM combined model, EMD-LSTM-GWO combined model, EEMD-LSTM-GWO
396 combined model and CEEMDAN-LSTM-GWO combined model. All WSF models are
397 applied to the data collected from the five wind farms shown in Fig. 3. The performance of
398 the models is measured by MAE, RMSE and MAPE performance indexes. The results of all

399 models for WSF are reported in Table 3 and Tables B.1-B.4. Also, the IMFs of ICEEMDAN,
400 which is used as the decomposition method in the creation of the developed ICEEMDAN-
401 LSTM-GWO combined model, and the ICEEMDAN-NAR hybrid model, ICEEMDAN-
402 NAR-GWO hybrid model and ICEEMDAN-LSTM hybrid model, are presented in Fig. 4 for
403 the WSTS collected from the five different wind farms. The performance of the models on
404 these test datasets are presented in Figs. 5-8 and Figs. B.1-B.16 in Appendix B. The
405 performance analysis for BOZ station is provided in the following; the analogous analysis of
406 the other stations is presented in the Appendix B.

407

408 For the dataset of BOZ station, the forecasting accuracy of the developed ICEEMDAN-
409 LSTM-GWO hybrid model for WSF has the best MAE, RMSE and MAPE at 0.1960, 0.2750
410 and 4.59%, respectively. Among the other individual and combined models considered, the
411 best five models are EEMD-LSTM-GWO, ICEEMDAN-LSTM, CEEMDAN-LSTM-GWO,
412 EEMD-LSTM and CEEMDAN-LSTM, with the lowest MAPE values of 5.74%, 5.83%,
413 5.93%, 7.09% and 7.47%, respectively. The five worst models are NAR, EMD-NAR-GWO,
414 ICEEMDAN-NAR-GWO, EMD-NAR and CEEMDAN-NAR-GWO, with the highest MAPE
415 values of 27.19%, 21.87%, 20.84%, 20.79% and 20.26%, respectively. The effect of
416 decomposition on the single model is shown in Figs. 5 and 6; the effect of GWO on the
417 combined models is shown in Figs. 7 and 8. Figs. 5-8 and Table 3 shows that ICEEMDAN-
418 LSTM-GWO is the best performing model. The results for the other four stations are similar
419 and detailed performance analyses are presented in the Appendix B.

420

421 In order to show that the proposed forecasting model is independent of the data set, the model
422 has been applied on the data obtained from IPS, GON, BAN, and SIL stations and
423 approximately the same forecasting performance has been obtained. When the developed
424 model is compared with some hybrid wind speed estimation studies [51-55] in the literature, it

425 is seen that the proposed method has a much better prediction performance. In addition to the
426 proposed signal processing method, well optimization of the weight coefficients in the LSTM
427 deep learning algorithm by the GWO algorithm plays an important role in this forecasting
428 performance.

429

Journal Pre-proof

430

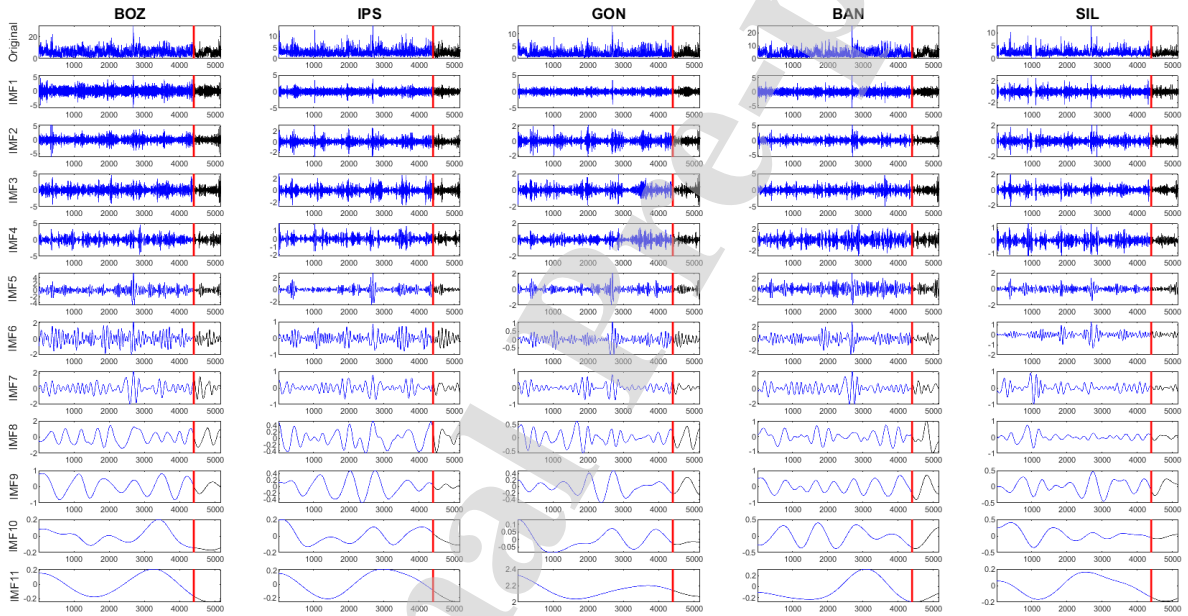
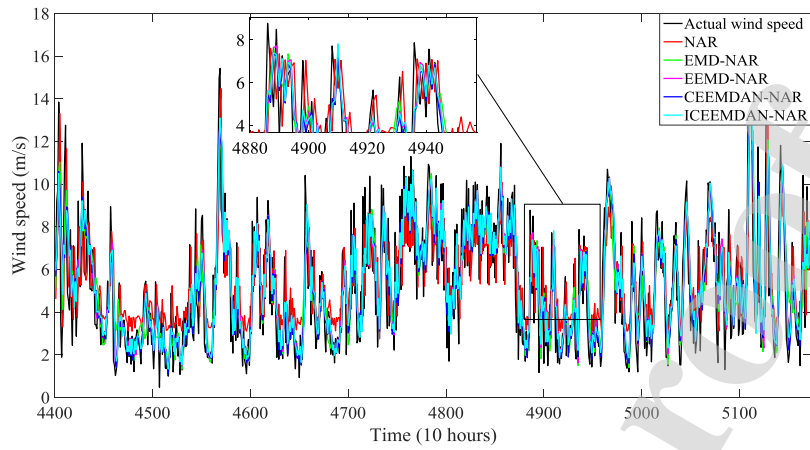


Fig. 4. IMFs of ICEEMDAN for WSTS gathered from the five stations.

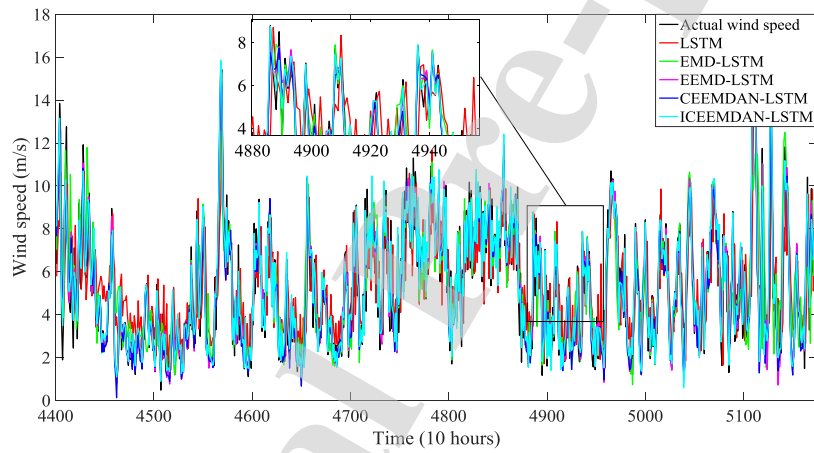
431
432



433
434

Fig. 5. WSF results achieved by using various NAR models for BOZ station.

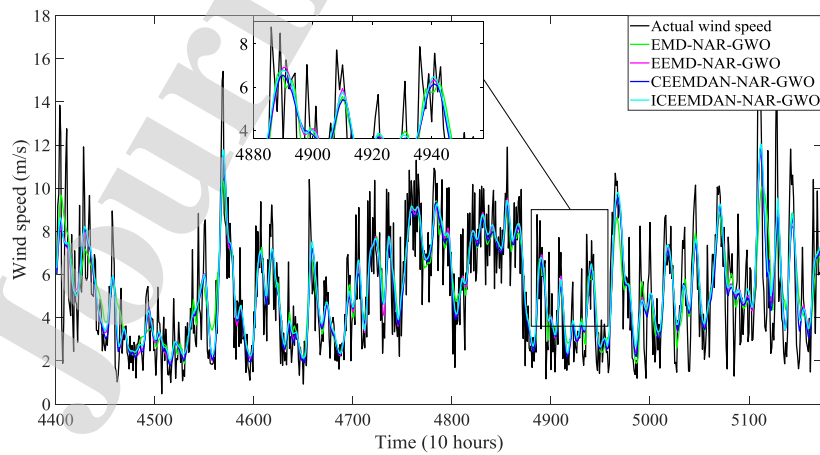
435



436
437

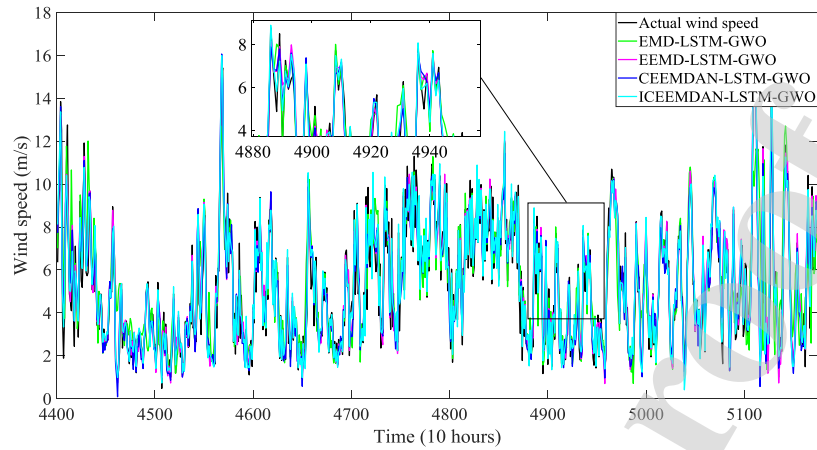
Fig. 6. WSF results achieved by using various LSTM models for BOZ station.

438



439
440

Fig. 7. WSF results achieved by using various NAR models with GWO for BOZ station.



441
442 **Fig. 8.** WSF results achieved by using various LSTM models with GWO for BOZ station.
443

444 **Table 3**

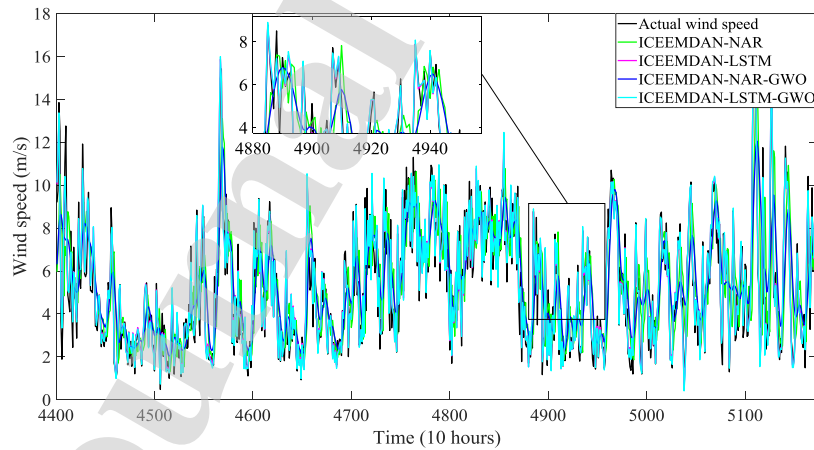
445 Comparison of various forecasting models for WSTS collected from BOZ station.

Models	MAE	RMSE	MAPE (%)
NAR	1.0080	1.2524	27.19
EMD-NAR	0.8314	1.1149	20.79
EEMD-NAR	0.7791	1.0408	19.13
CEEMDAN-NAR	0.6760	0.9137	16.35
ICEEMDAN-NAR	0.7469	1.0101	18.64
LSTM	0.6733	0.8641	18.06
EMD-LSTM	0.4629	0.6728	12.17
EEMD-LSTM	0.2962	0.3925	7.09
CEEMDAN-LSTM	0.3182	0.4131	7.47
ICEEMDAN-LSTM	0.2451	0.3409	5.83
EMD-NAR-GWO	0.8395	1.1079	21.87
EEMD-NAR-GWO	0.7898	1.0260	20.15
CEEMDAN-NAR-GWO	0.8052	1.0524	20.26
ICEEMDAN-NAR-GWO	0.7896	1.0240	20.84
EMD-LSTM-GWO	0.3758	0.5472	9.89
EEMD-LSTM-GWO	0.2366	0.3184	5.74
CEEMDAN-LSTM-GWO	0.2498	0.3286	5.93
ICEEMDAN- LSTM-GWO	0.1960	0.2750	4.59

446

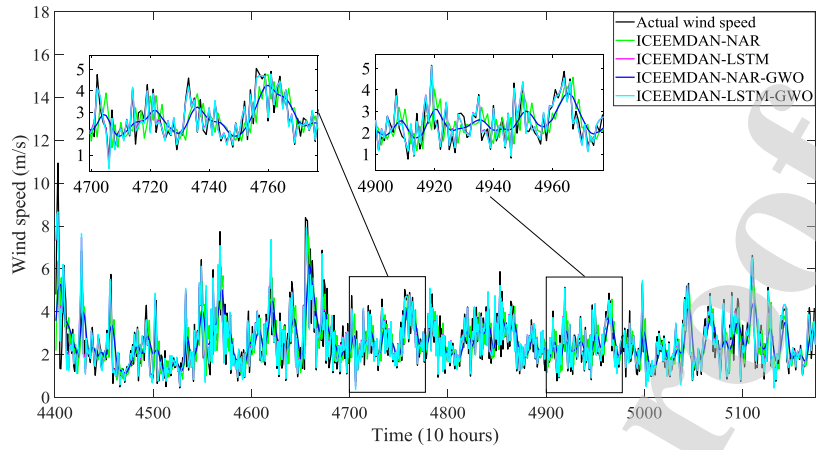
447 **4. Discussion**

448 The WF results of the ICEEMDAN-NAR, ICEEMDAN-LSTM, ICEEMDAN-NAR-GWO
 449 and ICEEMDAN-LSTM-GWO combined models created with the ICEEMDAN
 450 decomposition method are shown in Figs. 9-13 for each station. The mean of the performance
 451 index values for all models is presented in Table 4 for the five stations. The forecasting
 452 performance of the developed ICEEMDAN-LSTM-GWO hybrid WSF model has the best
 453 MAE, RMSE and MAPE compared to the other models, with values of 0.1309, 0.1847 and
 454 5.26%, respectively. The average MAPE values of ICEEMDAN-NAR, ICEEMDAN-LSTM
 455 and ICEEMDAN-NAR-GWO are 18.25%, 6.62% and 20.44%, respectively; the average
 456 MAE values of ICEEMDAN-NAR, ICEEMDAN-LSTM and ICEEMDAN-NAR-GWO are
 457 0.4575, 0.1635 and 0.4910, respectively; the average RMSE values of ICEEMDAN-NAR,
 458 ICEEMDAN-LSTM and ICEEMDAN-NAR-GWO are 0.6252, 0.2291 and 0.6384,
 459 respectively. It is clearly seen that the developed ICEEMDAN-LSTM-GWO hybrid WSF
 460 model performs better than the other models.



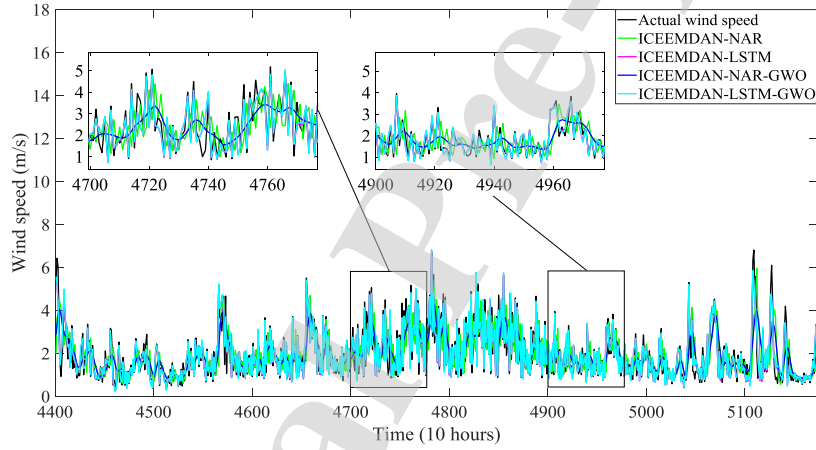
461
 462
 463
 464

Fig. 9. The best WSF results achieved by using various NAR and LSTM models for BOZ station.



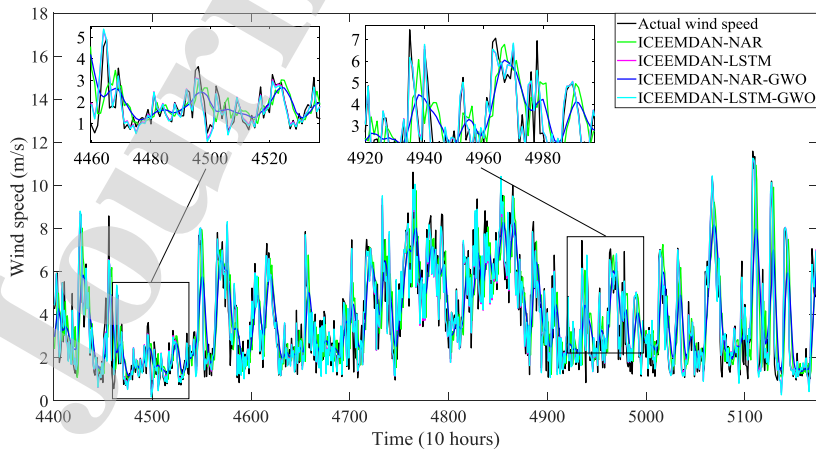
465
466
467
468
469

Fig. 10. The best WSF results achieved by using various NAR and LSTM models for IPS station.



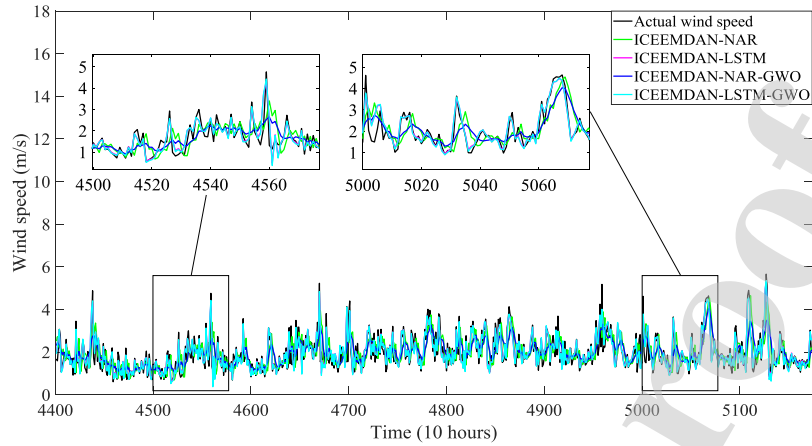
470
471
472
473

Fig. 11. The best WSF results achieved by using various NAR and LSTM models for GON station.



474
475
476

Fig. 12. The best WSF results achieved by using various NAR and LSTM models for BAN station.



477

478 **Fig. 13.** The best WSF results achieved by using various NAR and LSTM models for SIL
479 station.

480

481 **Table 4**

482 Comparison of the averages of the performance indexes for various forecasting models.

Models	MAE	RMSE	MAPE (%)
NAR	0.6351	0.8019	27.82
EMD-NAR	0.5060	0.6908	20.00
EEMD-NAR	0.4767	0.6449	19.09
CEEMDAN-NAR	0.4232	0.5736	17.01
ICEEMDAN-NAR	0.4575	0.6252	18.25
LSTM	0.4193	0.5489	17.76
EMD-LSTM	0.2688	0.3803	11.04
EEMD-LSTM	0.1852	0.2530	7.38
CEEMDAN-LSTM	0.1865	0.2529	7.34
ICEEMDAN-LSTM	0.1635	0.2291	6.62
EMD-NAR-GWO	0.5159	0.6758	21.47
EEMD-NAR-GWO	0.4935	0.6410	20.74
CEEMDAN-NAR-GWO	0.5048	0.6586	20.95
ICEEMDAN-NAR-GWO	0.4910	0.6384	20.44
EMD-LSTM-GWO	0.2192	0.3106	9.24
EEMD-LSTM-GWO	0.1484	0.2047	5.98
CEEMDAN-LSTM-GWO	0.1482	0.2028	5.91
ICEEMDAN-LSTM-GWO	0.1309	0.1847	5.26

483 It is seen that the performance of the models combined with signal processing methods is
484 better than the performance of single models. It is clear that signal processing methods
485 improve the performance of single models. The performance of the combined models with
486 LSTM appears to be better than that of the combined models with NAR. It can be said that the
487 performance of combined models with NAR is poor compared to the performance of single
488 LSTM models. In combination models with signal processing, models with EMD have the
489 worst performance. When the performance of the proposed forecasting model on the data sets
490 obtained from five stations is analyzed, it can be also concluded that it will show the same
491 forecasting performance on the data sets that are well known in wind speed forecasting.

492 5. Conclusions

493 WSF with high precision is quite important for efficient exploitation and usage of wind
494 energy. Uncertainty and non-stationarity of WS suggests the opportunity of employing
495 combined models for high precision and reliable WSF. In this paper, a hybrid model named
496 ICEEMDAN-LSTM-GWO, based on LSTM network and ICEEMDAN decomposition
497 method with GWO is developed for ST-WSF. Filling of missing data and smoothing of
498 WSTS data are performed by WMA in a preprocessing phase, followed by Z-score
499 normalization. The ICEEMDAN method is used in the decomposition phase and the models
500 created by using the ICEEMDAN method are compared with those created by using other
501 decomposition methods. The proposed ICEEMDAN-LSTM-GWO combined WSF model is
502 applied to data gathered from five wind stations in the Marmara region, Turkey. The obtained
503 experimental results demonstrate that the developed ICEEMDAN-LSTM-GWO combined
504 WSF model is superior to all other considered models.

505

506

507

508 **Appendix A**

509 ANN and AI forecasting models are used as single forecasting models without any
 510 decomposition or optimization algorithms. In this Appendix, the NAR forecasting model used
 511 to compare the performance of the developed ICEEMDAN-LSTM-GWO hybrid WSF model
 512 is described.

513

514 Recurrent neural networks, such as NAR, layer recurrent networks and time delay neural
 515 networks (TDNN) are widely used for modeling non-linear dynamic systems. The NAR
 516 neural network is defined as a feedback-driven and self-repeating network, including several
 517 layers [72]. The NAR model, which is widely used in time series predictions, is based on the
 518 linear AR model. The descriptive equation for a NAR neural network is:

$$\hat{y}(t) = f(y(t-1) + y(t-2) + \dots + y(t-d)) \quad (26)$$

519 where the subsequent values depend only on regressed d previous values of the output signal.

520 The non-linear function $f(\cdot)$ calculates the one-step ahead WS value by Eq. (26) depending
 521 on the previous one-step values of the output signal. The output of the closed loop NAR
 522 network is described as follows:

$$\hat{y}(t+p) = f(y(t-1) + y(t-2) + \dots + y(t-d)) \quad (27)$$

523 where p represents the forecasted steps in the future.

524

525

526

527

528

529

530

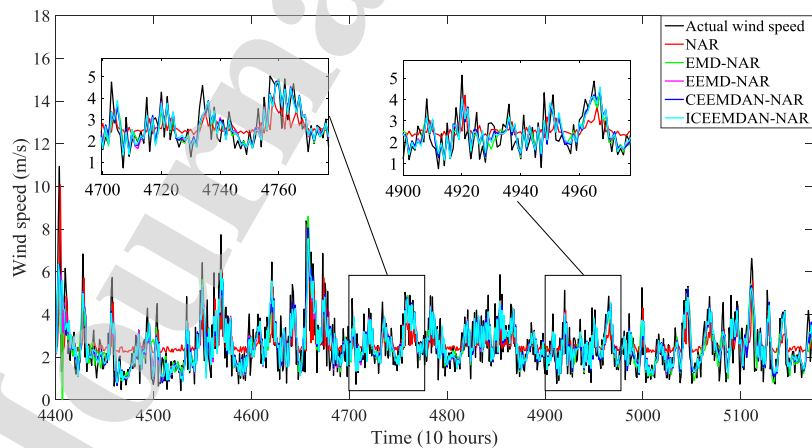
531 **Appendix B**

532 In this Appendix, the forecasting performance of the methods considered is performed with
 533 respect to the IPS, GON, BAN and SIL stations.

534

535 For IPS station, the forecasting performance of the developed ICEEMDAN-LSTM-GWO
 536 hybrid model for WSF has the lowest MAE, RMSE and MAPE values of 0.1289, 0.1878 and
 537 5.63%, respectively. Among the other individual and combined models considered, the best
 538 five models are CEEMDAN-LSTM-GWO, EEMD-LSTM-GWO, ICEEMDAN-LSTM,
 539 CEEMDAN-LSTM and EEMD-LSTM, with the lowest MAPE values of 6.40%, 6.70%,
 540 7.27%, 7.86% and 7.89%, respectively. The five worst models are NAR, EEMD-NAR-GWO,
 541 EMD-NAR-GWO, CEEMDAN-NAR-GWO and ICEEMDAN-NAR-GWO, with the highest
 542 MAPE values of 28.34%, 21.93%, 21.71%, 21.52% and 21.24%, respectively. The effect of
 543 decomposition on the single model is shown in Figs. B.1 and B.2; the effect of GWO on the
 544 combined models is shown in Figs. B.3 and B.4. Figs. B.1-B.4 and Table B.1 shows that
 545 ICEEMDAN-LSTM-GWO is the best performing model.

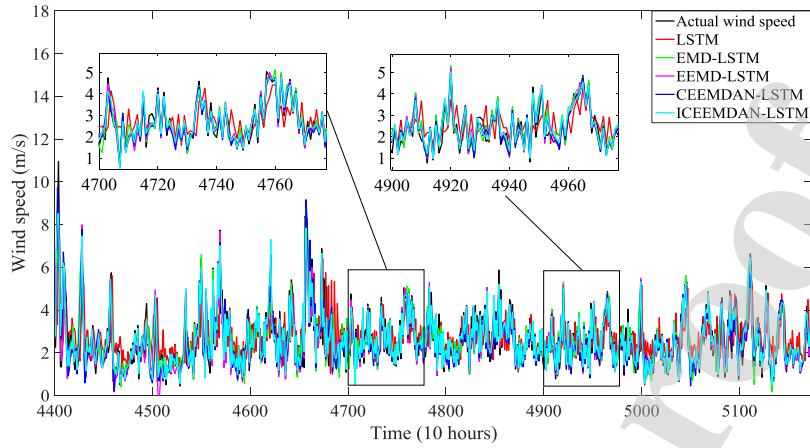
546



547

548 **Fig. B.1.** WSF results achieved by using various NAR models for IPS station.

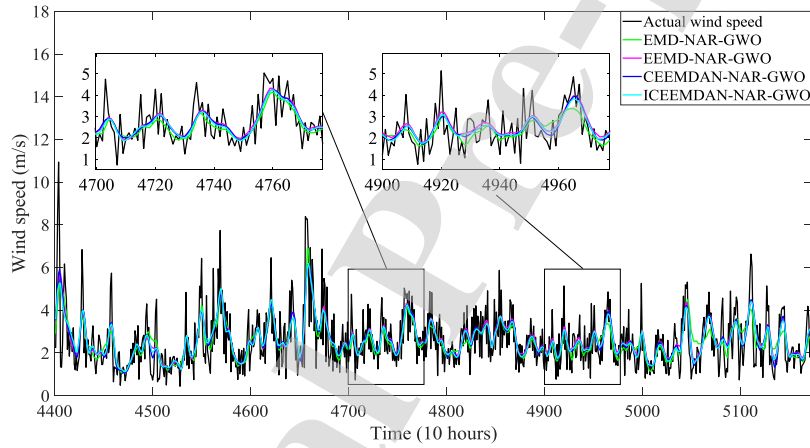
549



550
551

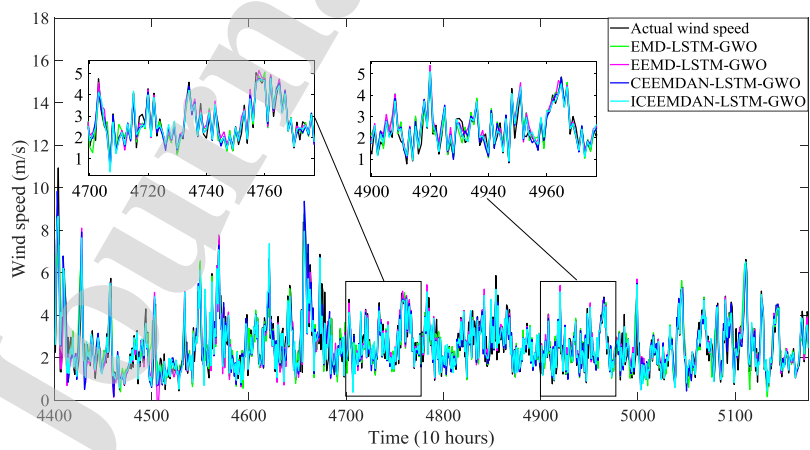
Fig. B.2. WSF results achieved by using various LSTM models for IPS station.

552



553
554

Fig. B.3. WSF results achieved by using various NAR models with GWO for IPS station.



555
556
557

Fig. B.4. WSF results achieved by using various LSTM models with GWO for IPS station.

558 **Table B.1.**

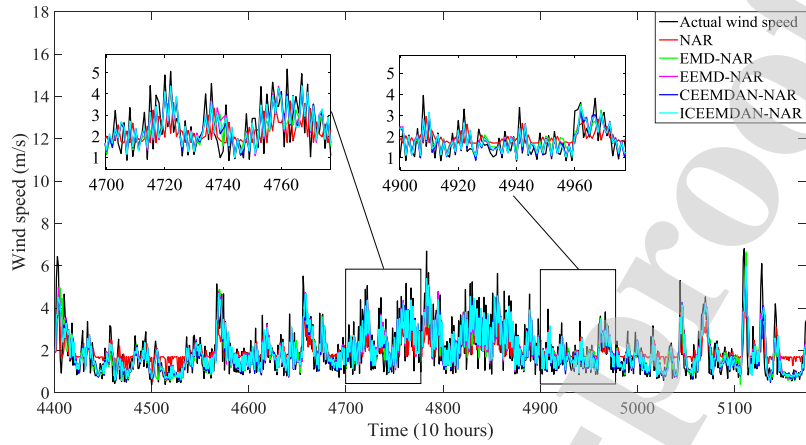
559 Comparison of various forecasting models for WSTS collected from IPS station.

Models	MAE	RMSE	MAPE (%)
NAR	0.5562	0.7148	28.34
EMD-NAR	0.4315	0.5904	20.35
EEMD-NAR	0.4220	0.5757	20.05
CEEMDAN-NAR	0.3682	0.5036	17.52
ICEEMDAN-NAR	0.4070	0.5695	19.24
LSTM	0.3789	0.5066	18.86
EMD-LSTM	0.2085	0.3016	10.21
EEMD-LSTM	0.1763	0.2522	7.89
CEEMDAN-LSTM	0.1718	0.2466	7.86
ICEEMDAN-LSTM	0.1626	0.2336	7.27
EMD-NAR-GWO	0.4529	0.5985	21.71
EEMD-NAR-GWO	0.4395	0.5777	21.93
CEEMDAN-NAR-GWO	0.4415	0.5836	21.52
ICEEMDAN-NAR-GWO	0.4344	0.5722	21.24
EMD-LSTM-GWO	0.1675	0.2431	8.14
EEMD-LSTM-GWO	0.1447	0.2065	6.70
CEEMDAN-LSTM-GWO	0.1391	0.2003	6.40
ICEEMDAN-LSTM-GWO	0.1289	0.1878	5.63

560

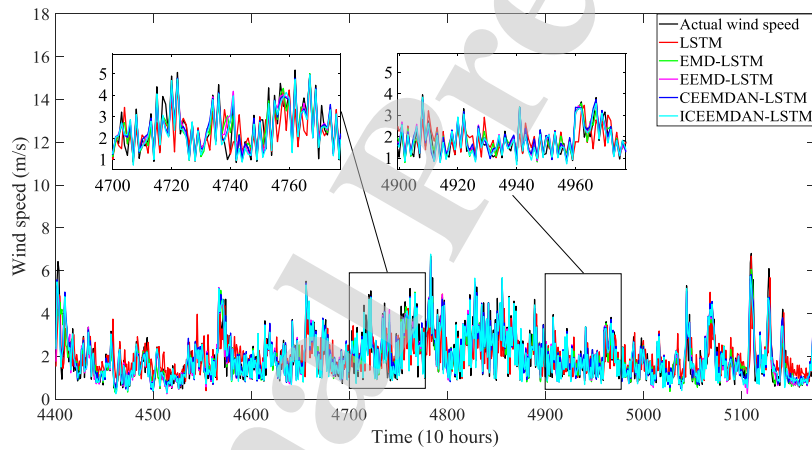
561 For GON station, the forecasting precision of the proposed ICEEMDAN-LSTM-GWO hybrid
 562 model for WSF has the lowest MAE, RMSE and MAPE values of 0.0930, 0.1364 and 5.63%,
 563 respectively. Among the other individual and combined models considered, the best five
 564 models are CEEMDAN-LSTM-GWO, EEMD-LSTM-GWO, ICEEMDAN-LSTM,
 565 CEEMDAN-LSTM and EEMD-LSTM, with the lowest MAPE values of 5.77%, 6.32%,
 566 6.88%, 7.49% and 7.92%, respectively. The five worst models are NAR, EMD-NAR-GWO,
 567 CEEMDAN-NAR-GWO, EEMD-NAR-GWO and ICEEMDAN-NAR-GWO, with the
 568 highest MAPE values of 33.82%, 25.10%, 24.20%, 24.12% and 23.48%, respectively. The
 569 effect of decomposition on the single model is shown in Figs. B.5 and B.6; the effect of GWO

570 on the combined models is shown in Figs. B.7 and B.8. Figs. B.5-B.8 and Table B.2 shows
 571 that ICEEMDAN-LSTM-GWO is the best performing model.



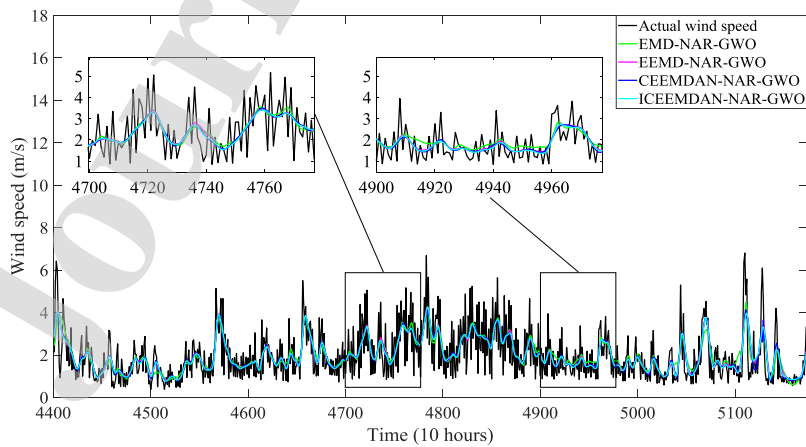
572
 573

Fig. B.5. WSF results achieved by using various NAR models for GON station.



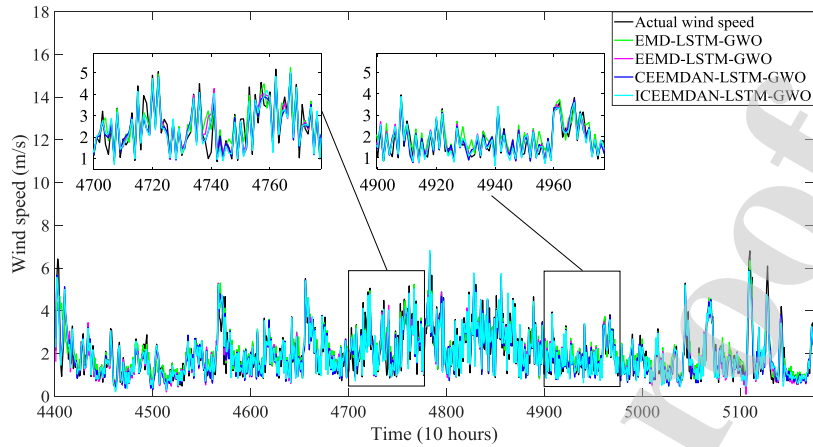
574
 575

Fig. B.6. WSF results achieved by using various LSTM models for GON station.



576
 577

Fig. B.7. WSF results achieved by using various NAR models with GWO for GON station.



578
579
580

Fig. B.8. WSF results achieved by using various LSTM models with GWO for GON station.

581 **Table B.2.**

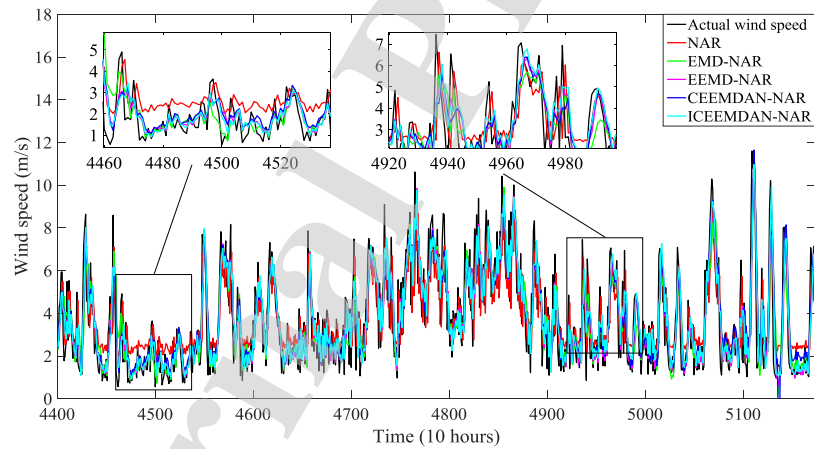
582 Comparison of various forecasting models for WSTS collected from GON station.

Models	MAE	RMSE	MAPE (%)
NAR	0.5164	0.6591	33.82
EMD-NAR	0.3688	0.5308	20.71
EEMD-NAR	0.3399	0.4737	20.09
CEEMDAN-NAR	0.3005	0.4219	17.36
ICEEMDAN-NAR	0.3257	0.4555	19.11
LSTM	0.2837	0.3778	18.07
EMD-LSTM	0.1670	0.2342	9.92
EEMD-LSTM	0.1341	0.1855	7.92
CEEMDAN-LSTM	0.1216	0.1751	7.49
ICEEMDAN-LSTM	0.1150	0.1691	6.88
EMD-NAR-GWO	0.4005	0.5165	25.10
EEMD-NAR-GWO	0.3868	0.4999	24.12
CEEMDAN-NAR-GWO	0.3946	0.5168	24.20
ICEEMDAN-NAR-GWO	0.3825	0.4977	23.48
EMD-LSTM-GWO	0.1427	0.1968	9.41
EEMD-LSTM-GWO	0.1078	0.1493	6.32
CEEMDAN-LSTM-GWO	0.0967	0.1394	5.77
ICEEMDAN-LSTM-GWO	0.0930	0.1364	5.63

583

584 For BAN station, the forecasting accuracy of the developed ICEEMDAN-LSTM-GWO
 585 hybrid model for WSF has the best MAE, RMSE and MAPE at 0.1503, 0.2026 and 5.73%,
 586 respectively. Among the other individual and combined models considered, the best five
 587 models are EEMD-LSTM-GWO, CEEMDAN-LSTM-GWO, ICEEMDAN-LSTM, EEMD-
 588 LSTM and CEEMDAN-LSTM, with the lowest MAPE values of 5.93%, 6.53%, 7.15%,
 589 7.54% and 7.75%, respectively. The five worst models are NAR, CEEMDAN-NAR-GWO,
 590 EMD-NAR-GWO, EEMD-NAR-GWO and ICEEMDAN-NAR-GWO, with the highest
 591 MAPE values of 29.72%, 23.76%, 23.39%, 22.95% and 22.59%, respectively. The effect of
 592 decomposition on the single model is shown in Figs. B.9 and B.10; the effect of GWO on the
 593 combined models is shown in Figs. B.11 and B.12. Figs. B.9-B.12 and Table B.3 shows that
 594 ICEEMDAN-LSTM-GWO is the best performing model.

595

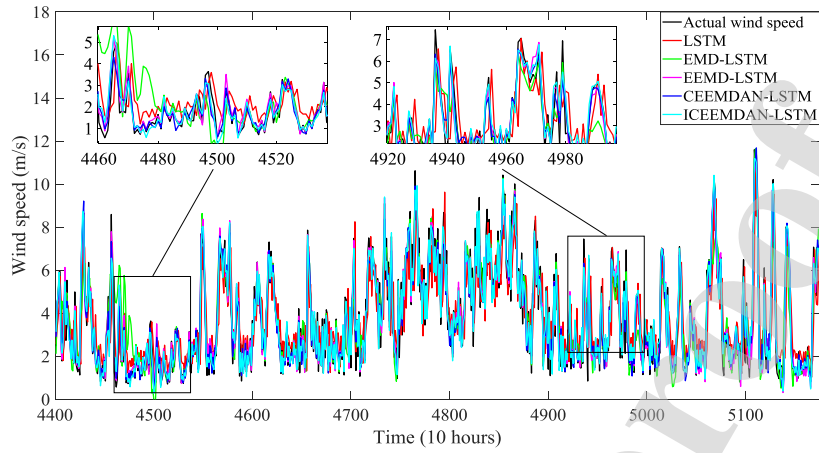


596

597

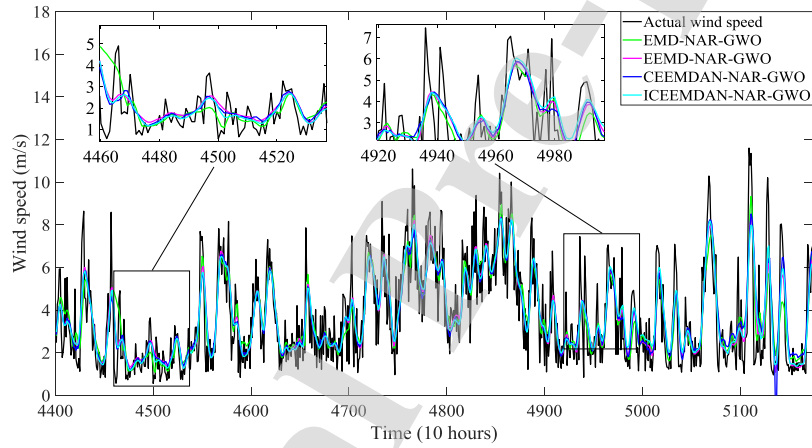
Fig. B.9. WSF results achieved by using various NAR models for BAN station.

598



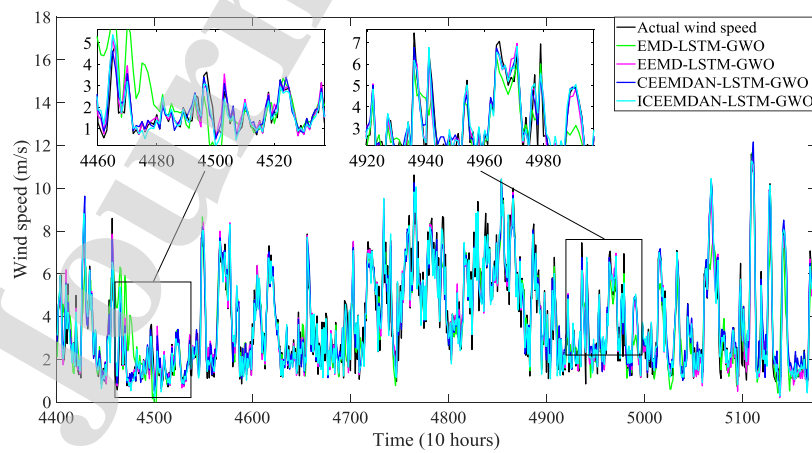
599
600
601

Fig. B.10. WSF results achieved by using various LSTM models for BAN station.



602
603
604

Fig. B.11. WSF results achieved by using various NAR models with GWO for BAN station.



605
606
607

Fig. B.12. WSF results achieved by using various LSTM models with GWO for BAN station.

608 **Table B.3.**

609 Comparison of various forecasting models for WSTS collected from BAN station.

Models	MAE	RMSE	MAPE (%)
NAR	0.7605	0.9548	29.72
EMD-NAR	0.6167	0.8377	22.52
EEMD-NAR	0.5730	0.7671	20.97
CEEMDAN-NAR	0.5346	0.7078	20.61
ICEEMDAN-NAR	0.5529	0.7415	20.11
LSTM	0.4977	0.6545	18.62
EMD-LSTM	0.3414	0.4677	13.69
EEMD-LSTM	0.2009	0.2687	7.54
CEEMDAN-LSTM	0.2112	0.2761	7.75
ICEEMDAN-LSTM	0.1871	0.2513	7.15
EMD-NAR-GWO	0.6125	0.8014	23.39
EEMD-NAR-GWO	0.5949	0.7642	22.95
CEEMDAN-NAR-GWO	0.6140	0.7881	23.76
ICEEMDAN-NAR-GWO	0.5953	0.7644	22.59
EMD-LSTM-GWO	0.2763	0.3818	11.06
EEMD-LSTM-GWO	0.1592	0.2157	5.93
CEEMDAN-LSTM-GWO	0.1675	0.2222	6.53
ICEEMDAN-LSTM-GWO	0.1503	0.2026	5.73

610

611

612

613

614

615

616

617

618 For SIL station, the forecasting performance of the proposed ICEEMDAN-LSTM-GWO
 619 hybrid model for WSF has the best MAE, RMSE and MAPE values at 0.0863, 0.1219 and
 620 4.74%, respectively. Among the other individual and combined models considered, the best
 621 five models are CEEMDAN-LSTM-GWO, EEMD-LSTM-GWO, ICEEMDAN-LSTM,
 622 CEEMDAN-LSTM and EEMD-LSTM, with the lowest MAPE values of 4.89%, 5.19%,
 623 5.98%, 6.13% and 6.45%, respectively. The five worst models are NAR, EMD-NAR, EMD-
 624 NAR-GWO, EEMD-NAR and LSTM, with the highest MAPE values of 20.01%, 15.61%,
 625 15.30%, 15.20% and 15.20%, respectively. The effect of decomposition on the single model
 626 is shown in Figs. B.13 and B.14; the effect of GWO on the combined models is shown in
 627 Figs. B.15 and B.16. Figs. B.13-B.16 and Table B.4 shows that ICEEMDAN-LSTM-GWO is
 628 the best performing model.

629

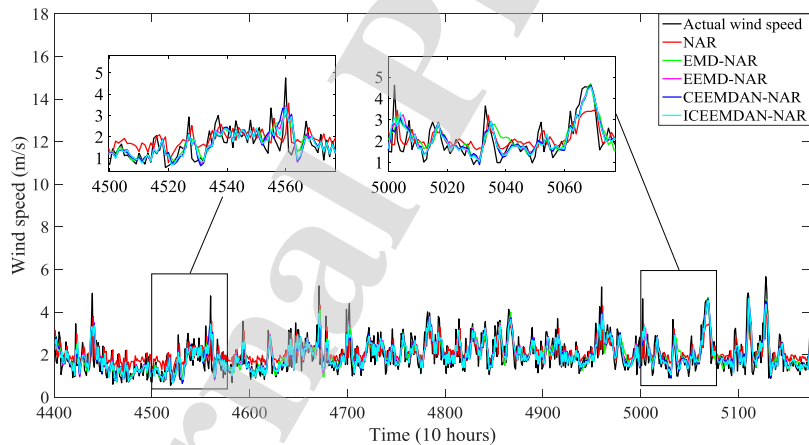
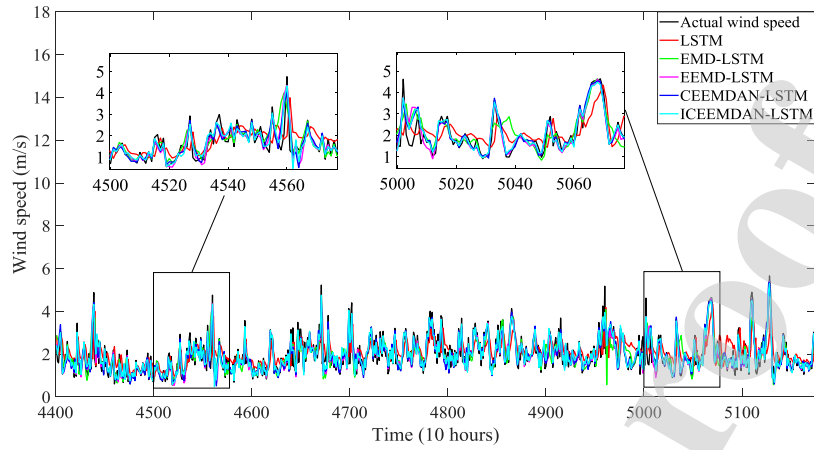
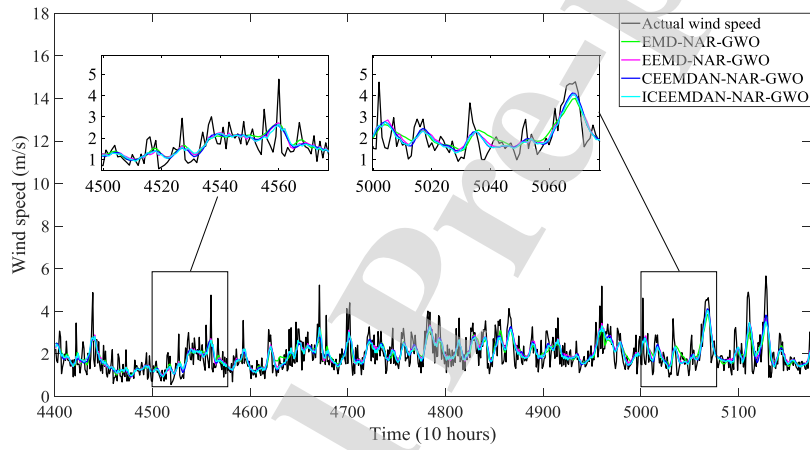
630
631

Fig. B.13. WSF results achieved by using various NAR models for SIL station.



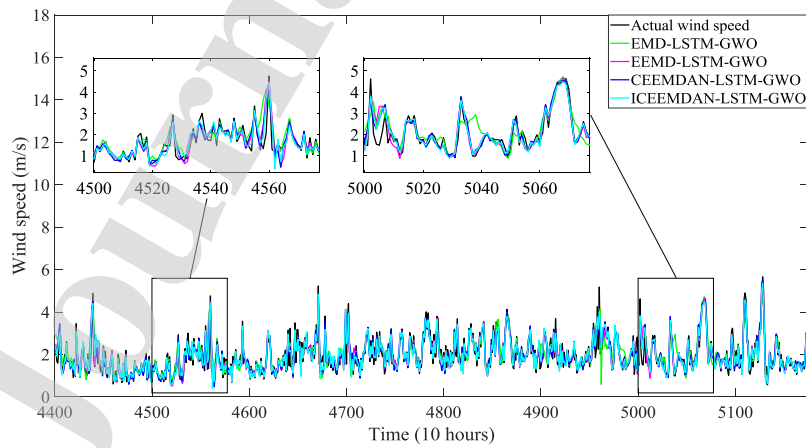
632
633

Fig. B.14. WSF results achieved by using various LSTM models for SIL station.



634
635

Fig. B.15. WSF results achieved by using various NAR models with GWO for SIL station.



637
638
639

Fig. B.16. WSF results achieved by using various LSTM models with GWO for SIL station.

640

641 **Table B.4.**

642 Comparison of various forecasting models for WSTS collected from SIL station.

Models	MAE	RMSE	MAPE (%)
NAR	0.3346	0.4282	20.01
EMD-NAR	0.2816	0.3800	15.61
EEMD-NAR	0.2694	0.3669	15.20
CEEMDAN-NAR	0.2367	0.3212	13.19
ICEEMDAN-NAR	0.2552	0.3492	14.16
LSTM	0.2630	0.3415	15.20
EMD-LSTM	0.1644	0.2254	9.19
EEMD-LSTM	0.1186	0.1659	6.45
CEEMDAN-LSTM	0.1098	0.1532	6.13
ICEEMDAN-LSTM	0.1079	0.1509	5.98
EMD-NAR-GWO	0.2742	0.3550	15.30
EEMD-NAR-GWO	0.2569	0.3369	14.56
CEEMDAN-NAR-GWO	0.2688	0.3521	15.00
ICEEMDAN-NAR-GWO	0.2535	0.3335	14.08
EMD-LSTM-GWO	0.1338	0.1842	7.69
EEMD-LSTM-GWO	0.0939	0.1337	5.19
CEEMDAN-LSTM-GWO	0.0877	0.1234	4.89
ICEEMDAN-LSTM-GWO	0.0863	0.1219	4.74

643

644

645

646

647

648

649

650

651

652 **References**

- 653 [1] IEA. Energy technology perspectives 2012. Pathways to a clean energy system. ISBN 978-92-64-17488-7.
654 2012.
- 655 [2] EC. Progress Reports. <<http://ec.europa.eu/energy/en/topics/renewable-energy/progress-reports>> 2016.
- 656 [3] Scarlat. N., Dallemand. J. F., Monforti-Ferrario. F., Banja. M., & Motola. V. (2015). Renewable energy
657 policy framework and bioenergy contribution in the European Union—An overview from National Renewable
658 Energy Action Plans and Progress Reports. *Renewable and Sustainable Energy Reviews*. 51. 969-985.
- 659 [4] World Wind Energy Association. Wind Power Capacity Worldwide Reaches 597 GW, 50, 1 GW added in
660 2018. [https://wwindea.org/blog/2019/02/25/wind-power-capacity-worldwide-reaches-600-gw-539-gw-added-in-](https://wwindea.org/blog/2019/02/25/wind-power-capacity-worldwide-reaches-600-gw-539-gw-added-in-2018)
661 2018 [accessed July 2019].
- 662 [5] Çakır. M. T.. "Türkiye'nin Rüzgâr Enerji Potansiyeli ve AB Ülkeleri İçindeki Yeri". *J. of Polytech.*, Vol.
663 13(4). 2010. p 287-293.
- 664 [6] Liu. H., Mi. X., & Li. Y. (2018). Smart deep learning based wind speed prediction model using wavelet
665 packet decomposition, convolutional neural network and convolutional long short term memory network. *Energy*
666 *Conversion and Management*. 166. 120-131.
- 667 [7] Li. H., Wang. J., Lu. H., & Guo. Z. (2018). Research and application of a combined model based on
668 variable weight for short term wind speed forecasting. *Renewable Energy*. 116. 669-684.
- 669 [8] Zhao. Y., Ye. L., Li. Z., Song. X., Lang. Y., & Su. J. (2016). A novel bidirectional mechanism based on
670 time series model for wind power forecasting. *Applied Energy*. 177. 793-803.
- 671 [9] Lei. M., Shiyan. L., Chuanwen. J., Hongling. L., & Yan. Z. (2009). A review on the forecasting of wind
672 speed and generated power. *Renewable and Sustainable Energy Reviews*. 13(4). 915-920.
- 673 [10] Bouzgou. H., & Benoudjit. N. (2011). Multiple architecture system for wind speed prediction. *Applied*
674 *Energy*. 88(7). 2463-2471.
- 675 [11] Cheng. W. Y., Liu. Y., Liu. Y., Zhang. Y., Mahoney. W. P., & Warner. T. T. (2013). The impact of model
676 physics on numerical wind forecasts. *Renewable Energy*. 55. 347-356.
- 677 [12] Dvorak. M. J., Archer. C. L., & Jacobson. M. Z. (2010). California offshore wind energy potential.
678 *Renewable Energy*. 35(6). 1244-1254.
- 679 [13] Carvalho. D., Rocha. A., Gómez-Gesteira. M., & Santos. C. (2012). A sensitivity study of the WRF model
680 in wind simulation for an area of high wind energy. *Environmental Modelling & Software*. 33. 23-34.
- 681 [14] Lazić. L., Pejanović. G., Živković. M., & Ilić. L. (2014). Improved wind forecasts for wind power
682 generation using the Eta model and MOS (Model Output Statistics) method. *Energy*. 73. 567-574.
- 683 [15] Al-Yahyai. S., Charabi. Y., & Gastli. A. (2010, December). Estimating wind resource over Oman using
684 meso-scale modeling. In *Energy Conference and Exhibition (EnergyCon), 2010 IEEE International* (pp. 536-
685 541). IEEE.
- 686 [16] Du. P., Wang. J., Guo. Z., & Yang. W. (2017). Research and application of a novel hybrid forecasting
687 system based on multi-objective optimization for wind speed forecasting. *Energy Conversion and Management*.
688 150. 90-107.
- 689 [17] Song. J., Wang. J., & Lu. H. (2018). A novel combined model based on advanced optimization algorithm
690 for short-term wind speed forecasting. *Applied Energy*. 215. 643-658.
- 691 [18] Poggi. P., Muselli. M., Notton. G., Cristofari. C., & Louche. A. (2003). Forecasting and simulating wind
692 speed in Corsica by using an autoregressive model. *Energy Conversion and Management*. 44(20). 3177-3196.

- 693 [19] Kani, S. P., Mousavi, S. M., Kaviani, A. K., & Riahy, G. H. (2008, October). A new integrated approach
694 for very short-term wind speed prediction using linear regression among ANN and Markov chain. In Proceeding
695 on International Conference on Power System Analysis, Control and Optimization.
- 696 [20] Riahy, G. H., & Abedi, M. (2008). Short term wind speed forecasting for wind turbine applications using
697 linear prediction method. *Renewable Energy*, 33(1), 35-41.
- 698 [21] Cassola, F., & Burlando, M. (2012). Wind speed and wind energy forecast through Kalman filtering of
699 Numerical Weather Prediction model output. *Applied Energy*, 99, 154-166.
- 700 [22] Zuluaga, C. D., Alvarez, M. A., & Giraldo, E. (2015). Short-term wind speed prediction based on robust
701 Kalman filtering: An experimental comparison. *Applied Energy*, 156, 321-330.
- 702 [23] Erdem, E., & Shi, J. (2011). ARMA based approaches for forecasting the tuple of wind speed and direction.
703 *Applied Energy*, 88(4), 1405-1414.
- 704 [24] Shamshad, A., Bawadi, M. A., Hussin, W. W., Majid, T. A., & Sanusi, S. A. M. (2005). First and second
705 order Markov chain models for synthetic generation of wind speed time series. *Energy*, 30(5), 693-708.
- 706 [25] Kavasseri, R. G., & Seetharaman, K. (2009). Day-ahead wind speed forecasting using f-ARIMA models.
707 *Renewable Energy*, 34(5), 1388-1393.
- 708 [26] Zhang, C., Wei, H., Zhao, X., Liu, T., & Zhang, K. (2016). A Gaussian process regression based hybrid
709 approach for short-term wind speed prediction. *Energy Conversion and Management*, 126, 1084-1092.
- 710 [27] Zhang, C., Zhou, J., Li, C., Fu, W., & Peng, T. (2017). A compound structure of ELM based on feature
711 selection and parameter optimization using hybrid backtracking search algorithm for wind speed forecasting.
712 *Energy Conversion and Management*, 143, 360-376.
- 713 [28] Karasu, S., Altan, A., Saraç, Z., & Hacıoğlu, R. (2017, May). Prediction of wind speed with non-linear
714 autoregressive (NAR) neural networks. In *Signal Processing and Communications Applications Conference*
715 (SIU), 2017 25th (pp. 1-4). IEEE.
- 716 [29] Cadenas, E., Rivera, W., Campos-Amezcuca, R., & Heard, C. (2016). Wind speed prediction using a
717 univariate ARIMA model and a multivariate NARX model. *Energies*, 9(2), 109.
- 718 [30] Karasu, S., Altan, A., Saraç, Z., & Hacıoğlu, R. (2017). Estimation of fast varied wind speed based on
719 NARX neural network by using curve fitting. *International Journal of Energy Applications and Technologies*,
720 4(3), 137-146.
- 721 [31] Maatallah, O. A., Achuthan, A., Janoyan, K., & Marzocca, P. (2015). Recursive wind speed forecasting
722 based on Hammerstein Auto-Regressive model. *Applied Energy*, 145, 191-197.
- 723 [32] Akçay, H., & Filik, T. (2017). Short-term wind speed forecasting by spectral analysis from long-term
724 observations with missing values. *Applied Energy*, 191, 653-662.
- 725 [33] Al-Dahidi, S., Baraldi, P., Zio, E., & Legnani, E. (2017, December). A dynamic weighting ensemble
726 approach for wind energy production prediction. In *2017 2nd International Conference on System Reliability and*
727 *Safety (ICSRS)* (pp. 296-302). IEEE.
- 728 [34] Ak, R., Li, Y. F., Vitelli, V., & Zio, E. (2018). Adequacy assessment of a wind-integrated system using
729 neural network-based interval predictions of wind power generation and load. *International Journal of Electrical*
730 *Power & Energy Systems*, 95, 213-226.
- 731 [35] Wang, S., Zhang, N., Wu, L., & Wang, Y. (2016). Wind speed forecasting based on the hybrid ensemble
732 empirical mode decomposition and GA-BP neural network method. *Renewable Energy*, 94, 629-636.
- 733 [36] Liu, H., Mi, X. W., & Li, Y. F. (2018). Wind speed forecasting method based on deep learning strategy
734 using empirical wavelet transform, long short term memory neural network and Elman neural network. *Energy*
735 *Conversion and Management*, 156, 498-514.

- 736 [37] Zhang. C.. Wei. H.. Xie. L.. Shen. Y.. & Zhang. K. (2016). Direct interval forecasting of wind speed using
737 radial basis function neural networks in a multi-objective optimization framework. *Neurocomputing*. 205. 53-63.
- 738 [38] Qian-Li. M.. Qi-Lun. Z.. Hong. P.. Tan-Wei. Z.. & Jiang-Wei. Q. (2008). Multi-step-prediction of chaotic
739 time series based on co-evolutionary recurrent neural network. *Chinese Physics B*. 17(2). 536.
- 740 [39] Liu. H.. Tian. H. Q.. Liang. X. F.. & Li. Y. F. (2015). Wind speed forecasting approach using secondary
741 decomposition algorithm and Elman neural networks. *Applied Energy*. 157. 183-194.
- 742 [40] Mehrkanoon, S. (2019). Deep shared representation learning for weather elements forecasting. *Knowledge-
743 Based Systems*, 179, 120-128.
- 744 [41] Xiao. L.. Shao. W.. Yu. M.. Ma. J.. & Jin. C. (2017). Research and application of a hybrid wavelet neural
745 network model with the improved cuckoo search algorithm for electrical power system forecasting. *Applied
746 Energy*. 198. 203-222.
- 747 [42] Damousis. I. G.. Alexiadis. M. C.. Theocharis. J. B.. & Dokopoulos. P. S. (2004). A fuzzy model for wind
748 speed prediction and power generation in wind parks using spatial correlation. *IEEE Transactions on Energy
749 Conversion*. 19(2). 352-361.
- 750 [43] Mohandes. M. A.. Halawani. T. O.. Rehman. S.. & Hussain. A. A. (2004). Support vector machines for
751 wind speed prediction. *Renewable Energy*. 29(6). 939-947.
- 752 [44] Guo. Z. H.. Wu. J.. Lu. H. Y.. & Wang. J. Z. (2011). A case study on a hybrid wind speed forecasting
753 method using BP neural network. *Knowledge-based systems*. 24(7). 1048-1056.
- 754 [45] Wang. J.. Yang. W.. Du. P.. & Niu. T. (2018). A novel hybrid forecasting system of wind speed based on a
755 newly developed multi-objective sine cosine algorithm. *Energy Conversion and Management*. 163. 134-150.
- 756 [46] Liu. H.. Mi. X.. & Li. Y. (2018). Smart multi-step deep learning model for wind speed forecasting based on
757 variational mode decomposition, singular spectrum analysis, LSTM network and ELM. *Energy Conversion and
758 Management*. 159. 54-64.
- 759 [47] Liu. H.. Mi. X.. & Li. Y. (2018). Comparison of two new intelligent wind speed forecasting approaches
760 based on wavelet packet decomposition. complete ensemble empirical mode decomposition with adaptive noise
761 and artificial neural networks. *Energy Conversion and Management*. 155. 188-200.
- 762 [48] Kiplangat. D. C.. Asokan. K.. & Kumar. K. S. (2016). Improved week-ahead predictions of wind speed
763 using simple linear models with wavelet decomposition. *Renewable Energy*. 93. 38-44.
- 764 [49] Zhou. J.. Shi. J.. & Li. G. (2011). Fine tuning support vector machines for short-term wind speed
765 forecasting. *Energy Conversion and Management*. 52(4). 1990-1998.
- 766 [50] Peng. T.. Zhou. J.. Zhang. C.. & Zheng. Y. (2017). Multi-step ahead wind speed forecasting using a hybrid
767 model based on two-stage decomposition technique and AdaBoost-extreme learning machine. *Energy
768 Conversion and Management*. 153. 589-602.
- 769 [51] Liu. D.. Niu. D.. Wang. H.. & Fan. L. (2014). Short-term wind speed forecasting using wavelet transform
770 and support vector machines optimized by genetic algorithm. *Renewable Energy*. 62. 592-597.
- 771 [52] Liu. H.. Wu. H.. & Li. Y. (2018). Smart wind speed forecasting using EWT decomposition. GWO
772 evolutionary optimization. RELM learning and IEWT reconstruction. *Energy Conversion and Management*. 161.
773 266-283.
- 774 [53] Chen. J.. Zeng. G. Q.. Zhou. W.. Du. W.. & Lu. K. D. (2018). Wind speed forecasting using nonlinear-
775 learning ensemble of deep learning time series prediction and extremal optimization. *Energy Conversion and
776 Management*. 165. 681-695.
- 777 [54] Hu. Y. L.. & Chen. L. (2018). A nonlinear hybrid wind speed forecasting model using LSTM network.
778 hysteretic ELM and Differential Evolution algorithm. *Energy Conversion and Management*. 173. 123-142.

- 779 [55] Wang, L., Li, X., & Bai, Y. (2018). Short-term wind speed prediction using an extreme learning machine
780 model with error correction. *Energy Conversion and Management*, 162, 239-250.
- 781 [56] Jiang, Y., & Huang, G. (2017). Short-term wind speed prediction: Hybrid of ensemble empirical mode
782 decomposition, feature selection and error correction. *Energy Conversion and Management*, 144, 340-350.
- 783 [57] Demirhan, H., & Renwick, Z. (2018). Missing value imputation for short to mid-term horizontal solar
784 irradiance data. *Applied Energy*, 225, 998-1012.
- 785 [58] Jain, A., Nandakumar, K., & Ross, A. (2005). Score normalization in multimodal biometric systems.
786 *Pattern Recognition*, 38(12), 2270-2285.
- 787 [59] Huang, N. E., Shen, Z., Long, S. R., Wu, M. C., Shih, H. H., Zheng, Q., ... & Liu, H. H. (1998, March). The
788 empirical mode decomposition and the Hilbert spectrum for nonlinear and non-stationary time series analysis. In
789 *Proceedings of the Royal Society of London A: mathematical, physical and engineering sciences* (Vol. 454, No.
790 1971, pp. 903-995). The Royal Society.
- 791 [60] Wu, Z., & Huang, N. E. (2009). Ensemble empirical mode decomposition: a noise-assisted data analysis
792 method. *Advances in adaptive data analysis*, 1(01), 1-41.
- 793 [61] Wu, Z. (2014). Ensemble empirical mode decomposition and its multi-dimensional extensions. In *Hilbert-
794 Huang Transform and Its Applications* (pp. 27-46).
- 795 [62] Torres, M. E., Colominas, M. A., Schlotthauer, G., & Flandrin, P. (2011, May). A complete ensemble
796 empirical mode decomposition with adaptive noise. In *Acoustics, speech and signal processing (ICASSP), 2011
797 IEEE international conference on* (pp. 4144-4147). IEEE.
- 798 [63] Colominas, M. A., Schlotthauer, G., & Torres, M. E. (2014). Improved complete ensemble EMD: A
799 suitable tool for biomedical signal processing. *Biomedical Signal Processing and Control*, 14, 19-29.
- 800 [64] Hochreiter, S., & Schmidhuber, J. (1997). Long short-term memory. *Neural Computation*, 9(8), 1735-1780.
- 801 [65] Li, Y., Wu, H., & Liu, H. (2018). Multi-step wind speed forecasting using EWT decomposition, LSTM
802 principal computing, RELM subordinate computing and IEWT reconstruction. *Energy Conversion and
803 Management*, 167, 203-219.
- 804 [66] He, F., Zhou, J., Feng, Z. K., Liu, G., & Yang, Y. (2019). A hybrid short-term load forecasting model based
805 on variational mode decomposition and long short-term memory networks considering relevant factors with
806 Bayesian optimization algorithm. *Applied Energy*, 237, 103-116.
- 807 [67] Mirjalili, S., Mirjalili, S. M., & Lewis, A. (2014). Grey wolf optimizer. *Advances in engineering software*,
808 69, 46-61.
- 809 [68] Muro, C., Escobedo, R., Spector, L., & Coppinger, R. P. (2011). Wolf-pack (*Canis lupus*) hunting strategies
810 emerge from simple rules in computational simulations. *Behavioural Processes*, 88(3), 192-197.
- 811 [69] Wang, X., Zhao, H., Han, T., Zhou, H., & Li, C. (2019). A grey wolf optimizer using Gaussian estimation
812 of distribution and its application in the multi-UAV multi-target urban tracking problem. *Applied Soft
813 Computing*, 78, 240-260.
- 814 [70] Tu, Q., Chen, X., & Liu, X. (2019). Multi-strategy ensemble grey wolf optimizer and its application to
815 feature selection. *Applied Soft Computing*, 76, 16-30.
- 816 [71] Acar, M. S., Erbas, O., & Arslan, O. (2019). The performance of vapor compression cooling system aided
817 Ranque-Hilsch vortex tube. *Thermal Science*, 23(2 Part B), 1189-1201.
- 818 [72] Benmouiza, K., & Chekane, A. (2016). Small-scale solar radiation forecasting using ARMA and nonlinear
819 autoregressive neural network models. *Theoretical and Applied Climatology*, 124(3-4), 945-958.

HIGHLIGHTS

- A novel combined model based on long short-term memory neural network and decomposition methods with grey wolf optimizer algorithm is successfully proposed.
- The proposed combined model will significantly improve the forecasting accuracy.
- The effectiveness of the proposed combined model is tested on data from the wind farm in five regions.
- The experimental results indicate that the proposed combined wind speed forecasting model can capture non-linear features of the wind speed time series.

Author contributions

Use this form to specify the contribution of each author of your manuscript. A distinction is made between five types of contributions: Conceived and designed the analysis; Collected the data; Contributed data or analysis tools; Performed the analysis; Wrote the paper.

For each author of your manuscript, please indicate the types of contributions the author has made. An author may have made more than one type of contribution. Optionally, for each contribution type, you may specify the contribution of an author in more detail by providing a one-sentence statement in which the contribution is summarized. In the case of an author who contributed to performing the analysis, the author's contribution for instance could be specified in more detail as 'Performed the computer simulations', 'Performed the statistical analysis', or 'Performed the text mining analysis'.

If an author has made a contribution that is not covered by the five pre-defined contribution types, then please choose 'Other contribution' and provide a one-sentence statement summarizing the author's contribution.

Manuscript title: A new hybrid model for wind speed forecasting combining long short-term memory neural network, decomposition methods and grey wolf optimizer

Author 1: Aytaç Altan

- Conceived and designed the analysis**
Specify contribution in more detail (optional; no more than one sentence)
- Collected the data**
Specify contribution in more detail (optional; no more than one sentence)
- Contributed data or analysis tools**
Specify contribution in more detail (optional; no more than one sentence)
- Performed the analysis**
Specify contribution in more detail (optional; no more than one sentence)
- Wrote the paper**
Specify contribution in more detail (optional; no more than one sentence)
- Other contribution**
Specify contribution in more detail (required; no more than one sentence)

Author 2: Seçkin Karasu

- Conceived and designed the analysis**
Specify contribution in more detail (optional; no more than one sentence)
- Collected the data**
Specify contribution in more detail (optional; no more than one sentence)
- Contributed data or analysis tools**
Specify contribution in more detail (optional; no more than one sentence)
- Performed the analysis**
Specify contribution in more detail (optional; no more than one sentence)
- Wrote the paper**
Specify contribution in more detail (optional; no more than one sentence)
- Other contribution**
Specify contribution in more detail (required; no more than one sentence)

Author 3: Enrico Zio

- Conceived and designed the analysis**
Specify contribution in more detail (optional; no more than one sentence)
- Collected the data**
Specify contribution in more detail (optional; no more than one sentence)
- Contributed data or analysis tools**
Specify contribution in more detail (optional; no more than one sentence)
- Performed the analysis**
Specify contribution in more detail (optional; no more than one sentence)
- Wrote the paper**
Specify contribution in more detail (optional; no more than one sentence)
- Other contribution**
Specify contribution in more detail (required; no more than one sentence)

Author 4: Enter author name

- Conceived and designed the analysis**
Specify contribution in more detail (optional; no more than one sentence)
- Collected the data**
Specify contribution in more detail (optional; no more than one sentence)
- Contributed data or analysis tools**
Specify contribution in more detail (optional; no more than one sentence)
- Performed the analysis**
Specify contribution in more detail (optional; no more than one sentence)
- Wrote the paper**
Specify contribution in more detail (optional; no more than one sentence)
- Other contribution**
Specify contribution in more detail (required; no more than one sentence)

Author 5: Enter author name

- Conceived and designed the analysis**
Specify contribution in more detail (optional; no more than one sentence)
- Collected the data**
Specify contribution in more detail (optional; no more than one sentence)
- Contributed data or analysis tools**
Specify contribution in more detail (optional; no more than one sentence)
- Performed the analysis**
Specify contribution in more detail (optional; no more than one sentence)
- Wrote the paper**
Specify contribution in more detail (optional; no more than one sentence)
- Other contribution**
Specify contribution in more detail (required; no more than one sentence)

Author 6: Enter author name

- Conceived and designed the analysis**
Specify contribution in more detail (optional; no more than one sentence)
- Collected the data**
Specify contribution in more detail (optional; no more than one sentence)
- Contributed data or analysis tools**
Specify contribution in more detail (optional; no more than one sentence)
- Performed the analysis**
Specify contribution in more detail (optional; no more than one sentence)
- Wrote the paper**
Specify contribution in more detail (optional; no more than one sentence)
- Other contribution**
Specify contribution in more detail (required; no more than one sentence)

Author 7: Enter author name

- Conceived and designed the analysis**
Specify contribution in more detail (optional; no more than one sentence)
- Collected the data**
Specify contribution in more detail (optional; no more than one sentence)
- Contributed data or analysis tools**
Specify contribution in more detail (optional; no more than one sentence)
- Performed the analysis**
Specify contribution in more detail (optional; no more than one sentence)
- Wrote the paper**
Specify contribution in more detail (optional; no more than one sentence)
- Other contribution**
Specify contribution in more detail (required; no more than one sentence)

Author 8: Enter author name

- Conceived and designed the analysis**
Specify contribution in more detail (optional; no more than one sentence)
- Collected the data**
Specify contribution in more detail (optional; no more than one sentence)
- Contributed data or analysis tools**
Specify contribution in more detail (optional; no more than one sentence)
- Performed the analysis**
Specify contribution in more detail (optional; no more than one sentence)
- Wrote the paper**
Specify contribution in more detail (optional; no more than one sentence)
- Other contribution**
Specify contribution in more detail (required; no more than one sentence)

Author 9: Enter author name

- Conceived and designed the analysis**
Specify contribution in more detail (optional; no more than one sentence)
- Collected the data**
Specify contribution in more detail (optional; no more than one sentence)
- Contributed data or analysis tools**
Specify contribution in more detail (optional; no more than one sentence)
- Performed the analysis**
Specify contribution in more detail (optional; no more than one sentence)
- Wrote the paper**
Specify contribution in more detail (optional; no more than one sentence)
- Other contribution**
Specify contribution in more detail (required; no more than one sentence)

Author 10: Enter author name

- Conceived and designed the analysis**
Specify contribution in more detail (optional; no more than one sentence)
- Collected the data**
Specify contribution in more detail (optional; no more than one sentence)
- Contributed data or analysis tools**
Specify contribution in more detail (optional; no more than one sentence)
- Performed the analysis**
Specify contribution in more detail (optional; no more than one sentence)
- Wrote the paper**
Specify contribution in more detail (optional; no more than one sentence)
- Other contribution**
Specify contribution in more detail (required; no more than one sentence)

Declaration of interests

The authors declare that they have no known competing financial interests or personal relationships that could have appeared to influence the work reported in this paper.

The authors declare the following financial interests/personal relationships which may be considered as potential competing interests:

Journal Pre-proof